공학박사학위논문

Nucleic Acid Extraction Method and Microfluidic Device for Molecular Diagnostics

분자진단을 위한 핵산 추출 방법 및 미세유체 디바이스

2013 년 2 월

서울대학교 대학원

협동과정 바이오엔지니어링전공

황 규 연

Nucleic Acid Extraction Method and Microfluidic Device for Molecular Diagnostics

분자진단을 위한 핵산 추출 방법 및 미세유체 디바이스

지도교수 서 갑 양

이 논문을 공학박사 학위논문으로 제출함

2012 년 10 월

서울대학교 대학원

협동과정 바이오엔지니어링전공

황 규 연

황규연의 공학박사 학위논문을 인준함

2012 년 12 월

위 원 장 박 태 현 (인)

부 위 원 장 서 갑 양 (인)

위 원 전 누 리 (인)

위 원 김 영 록 (인)

위 원 김 준 호 (인)

Abstract

A novel bacterial DNA extraction method with microfluidic device has been developed for molecular diagnostics. In order to incorporate the conventional complex DNA sample preparation processes into microdevice, a solid phase DNA extraction composed of bacterial cell capture, washing, *in-situ* lysis, DNA elution was attempted, and it demonstrated that the full process of pathogen capture to DNA isolation from various human specimens could be automated in a single microchip.

At first, to facilitate the bacterial cell capture onto the solid surface of flow-through microdevice, the thermodynamically-favorable conditions for bacterial adhesion such as surface tension of solid surface and medium pH were optimized. The surface-modified silicon pillar arrays for bacterial cell capture were fabricated and their ability to capture bacterial cells was demonstrated. The capture efficiency for bacterial cells such as *E. coli*, *S. epidermis* and *S. mutans* in buffer solution was over 75% with a flow rate of 400 μL/min. Moreover, the proposed method captured *E. coli* cells present in 50% whole blood effectively. The captured cells from whole blood were then *in-situ* lyzed on the surface of the microchip and the eluted DNA was successfully amplified by polymerase chain reaction (PCR).

Next, in order to manufacture a low-cost, disposable microchip, micropillar arrays of high surface-to-volume ratio (SVR, 0.152 μm^{-1}) were constructed on polymethyl methacrylate (PMMA) by hot embossing with an electroformed Ni mold, and their

surface was modified with SiO_2 and an organosilane compound in subsequent steps. To seal open microchannels, the organosilane layer on top plane of the micropillars was selectively removed through photocatalytic oxidation *via* TiO_2/UV treatment at room temperature. As a result, the underlying SiO_2 surface was exposed without deteriorating the organosilane layer coated on lateral surface of the micropillars that could serve as bacterial cell adhesion moiety. Afterwards, a plasma-treated polydimethylsiloxane (PDMS) substrate was bonded to the exposed SiO_2 surface, completing the device fabrication. To optimize manufacturing throughput and process integration, the whole fabrication process was performed at 6 inch wafer-level including polymer imprinting, organosilane coating, and bonding. Preparation of bacterial DNA was carried out from urine samples with the fabricated PDMS/PMMA chip according to the suggested procedure: bacterial cell capture, washing, *in-situ* lysis, and DNA elution. The polymer-based microchip presented here demonstrated similar performance to Glass/Si chip in terms of bacterial cell capture efficiency and PCR compatibility.

And then, a miniaturized bead-beating device has been developed to automate nucleic acids extraction from gram-positive bacteria. The microfluidic device was fabricated by sandwiching a monolithic flexible PDMS membrane between two glass wafers (*i.e.*, glass-PDMS-glass), which acted as an actuator for bead collision *via* its pneumatic vibration without additional lysis equipment. The gram-positive bacteria, *S. aureus* and methicillin-resistant *S. aureus* (MRSA), were captured on surface-modified glass beads from 1 mL of initial sample solution and *in-situ* lyzed by bead-beating operation. Then,

10 μL or 20 μL of bacterial DNA solution was eluted and amplified successfully by real-time PCR. It was found that liquid volume faction played a crucial role in determining the cell lysis efficiency in a confined chamber by facilitating membrane deflection and bead motion. The miniaturized bead-beating operation disrupted most of *S. aureus* within 3 min, which turned out to be as efficient as the conventional benchtop vortexing machine or enzyme-based lysis technique. The effective cell concentration was significantly enhanced with the reduction of initial sample volume by 50 or 100 times. Combination of such analyte enrichment and *in-situ* bead-beating lysis provided an excellent PCR detection sensitivity amounting to *ca.* 46 CFU even for the gram-positive bacteria.

Finally, such a bead-packed microfluidic device with a built-in flexible wall was further applied to automate extraction of nucleic acids from MRSA in nasal swab. The flexible PDMS membrane was designed to manipulate the SVR of bead-packed chamber in the range of 0.05 to 0.15 (μm^{-1}) for a typical solid phase extraction protocol composed of binding, washing, and eluting. In particular, the pneumatically-assisted close packing of beads led to an invariant SVR (0.15 μm^{-1}) even with different bead amounts (10 ~ 16 mg), which allowed for consistent operation of the device and improved capture efficiency for bacteria cells. Furthermore, vigorous mixing by asynchronous membrane vibration enabled *ca.* 90% DNA recovery with *ca.* 10 μL of liquid solution from the captured cells on the bead surfaces. The full processes to detect MRSA in nasal swab, *i.e.*, nasal swab collection, pre-filtration, on-chip DNA extraction, and real-time PCR amplification were successfully constructed and carried out to validate the capability to

detect MRSA in nasal swab samples. This flexible microdevice provided an excellent analytical PCR detection sensitivity of *ca.* 61 CFU/swab with 95% confidence interval, which turned out to be higher than or similar to that of the commercial DNA-based MRSA detection techniques. This excellent performance would be attributed to the capability of the flexible bead-packed microdevice to enrich the analyte from a large initial sample (*e.g.*, 1 mL) into a microscale volume of eluate (*e.g.*, 10 μL). The proposed microdevice will find many applications as a solid phase extraction method toward various sample-to-answer systems.

Key Words : Solid phase extraction, Cell capture, Surface-modified, Flow-through, Bead-beating lysis, Surface-to-volume ratio, Flexible bead-packed microdevice

Student Number: 2009-30955

Contents

List of Tables

List of Figures

centrifugation and subsequent table-top bead-beating lysis with 10 µL of NaOH solution. 4 µL of DNA solution was included in PCR as template. Three repetitions were performed for each condition.

Chapter 1. Introduction

Nucleic acid-based micro total analysis system (μTAS) or Lab-On-a-Chip (LOC) is a promising molecular diagnosis approach since entire analytical procedures (*i.e.*, sample preparation, amplification, and detection) are integrated and automated on a microchip format (Figure 1-1). Real-time polymerase chain reaction (RT-PCR) has been widely accepted as both amplification and detection techniques because it provides higher accuracy and wider dynamic range than conventional PCR by determining the threshold cycle (Ct) directly proportional to the initial copy number. Moreover, it facilitates the integration of PCR technique into a microfluidic system by removing post-PCR processes such as sample transfer, reagent addition, gel-electrophoresis and fluorescence imaging. However, DNA sample preparation process to acquire PCR-quality DNA from the raw samples remains as a critical hurdle toward the integration of full analytical steps into μTAS. In order to achieve the successful amplification, nucleic acids should be properly extracted from clinical samples without potential PCR inhibitors because they have a direct effect on PCR performance (*i.e.*, sensitivity and specificity). In addition, it is highly desirable to have the capability of enriching target analyte from a large volume of initial sample (*e.g.*, mL) into a microchamber during the sample preparation processes. By doing so, the large sample volume will be properly interfaced with micro-scaled devices, which can increase the detection sensitivity through target analyte concentration. This

would be one of the most important characteristics of μTAS which can compete with the conventional benchtop analytical methods. Therefore, incorporation of the above functions into the nucleic acid sample preparation device would be the key to the practical application of μTAS.

In *Chapter 2*, we report a flow-through type microdevice capable of processing large sample volume to capture bacterial cells. To do this, the thermodynamically-favorable conditions for bacterial adhesion onto the solid surface were optimized by controlling the surface tension of the chip substrate and the media pH. On the basis of observed results, pillar arrays were fabricated to increase the surface-to-volume ratio (SVR) and enhance bacterial cell adhesion. Our microchip showed outstanding bacterial cell capture efficiency in buffer solution and more importantly even in 50% whole blood. Furthermore, we demonstrated an *in-situ* DNA extraction from captured cells and evaluated the prepared DNA quality in comparison with commercially available Qiagen kit.

In *Chapter 3*, we report a fabrication method to replace inorganic substrates with much cheaper polymer materials. Micropillar arrays on polymethylmethacrylate (PMMA) substrate were generated by hot embossing technique with an electroformed Ni mold, and organosilane was coated following room temperature deposition of SiO_2. Finally, the processed PMMA substrate was bonded to polydimethylsiloxane (PDMS) sheet to enclose the microchannels. PDMS is a well-known polymeric material that has been

widely used in various microfluidic devices. In particular, bonding characteristic of PDMS to a variety of hydrophilic inorganic oxide materials such as SiO_2 are attractive in that only surface activation is required without the use of adhesives or solvents. To facilitate PDMS-interface bonding to organosilane-modified SiO_2 surface, photocatalyst was employed to selectively remove a thin organosilane film on top plane of the micropillars without any adverse effects on their lateral surface. This approach allowed us to fabricate a low-cost plastic microchip without loss of bioanalytical activities such as bacterial cell capture and PCR compatibility.

In *Chapter 4*, we report a bead-beating microdevice through the pneumatic vibration of elastomeric membrane (PDMS). It was fabricated by sandwiching a PDMS membrane between two glass chips (glass-PDMS-glass). In order to automate the full DNA extraction processes efficiently, the proposed microdevice and biological protocol were designed to have the following features: First, a monolithic flexible PDMS membrane, typically used as a flow-regulating tool, was further employed as an actuator for bead collision *via* its pneumatic vibration. Namely, both manipulation of solutions (pumping and valving) and bead-beating for mechanical cell lysis were simultaneously implemented on a microchip using a single pneumatic source without any specialized lysis equipments. Also, valve seat and weir for bead trapping were designed to have the same microstructure, thereby simplifying the overall fabrication processes. In the aspect of biological protocol, surface-modified glass beads were used to capture bacterial cells,

which also acted as a grinding media to disrupt the captured cells on their surface. Furthermore, the present microdevice transformed the captured cells from 1 mL of initial sample into an analyte volume of 10 or 20 μL DNA solution. It reduced the initial sample volume by 100 or 50-fold, thereby concentrating the target analyte into a microscale volume that is more compatible for subsequent PCR amplification. As a result, our microdevice showed an excellent DNA extraction performance similar to the conventional benchtop vortexing machine or enzymatic method, allowing for successful PCR detection of gram-positive bacteria.

In *Chapter 5*, we report that such a bead-beating platform can be significantly improved by adjusting the SVR for each solid phase extraction step. More importantly, the analytical validation on this platform is attempted by detecting MRSA strains in nasal swab samples. The present bead-packed chamber has a flexible PDMS wall to control its void volume. Such flexibility allows for reversible switching of the two packing states between random close packing (*i.e.*, high SVR) and loose packing (*i.e.*, low SVR) by deflecting the flexible wall upwards or downwards. Also, the cycling of these two states could induce vigorous mixing and disrupt the cell membrane even for gram-positive bacteria. Interestingly, the close packing of beads was highly reproducible and consistent (*i.e.*, invariant SVR) even with different bead amounts (10 ~ 16 mg). These additional dynamic characteristics to a typical stationary solid phase enabled the proposed microdevice to be more suitable for a series of solid phase extraction steps (binding-

washing-eluting). By taking advantage of the above features, the analytical performance was evaluated by constructing the full detection schemes for MRSA detection in nasal swab, such as nasal swab collection, pre-filtration for the removal of large impurities, on-chip DNA extraction, and real-time PCR. The current flexible microdevice yielded an excellent analytical PCR detection sensitivity of *ca.* 61 CFU/swab with 95% confidence interval, which was comparable to the commercial MRSA detection techniques.

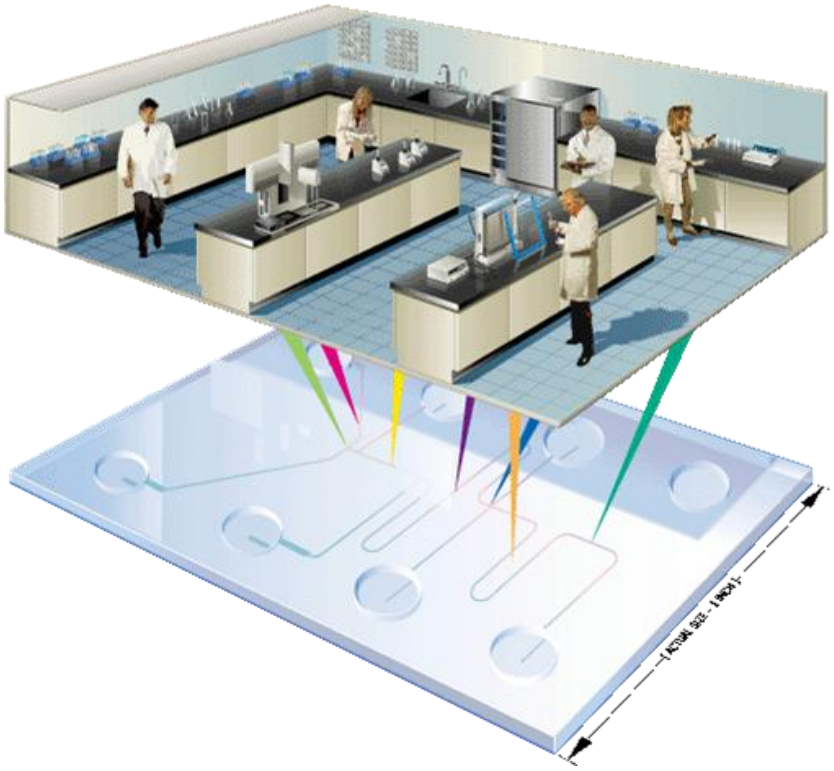

Figure 1-1. Conceptual image of LOC (Lab-On-a-Chip) or μTAS (micro total analysis system). Image capture from the website, http://www.mines.polito.it.

Chapter 2. Bacterial DNA extraction using surface-modified Si pillar arrays

2-1. Introduction

Lab-on-a-chip (LOC) or micro total analysis system (μTAS) is a promising approach to fully automate clinical molecular diagnostic tests. LOC often deals with picoliter to microliter sample volumes and attempts to analyze samples on the order of a few minutes [1-3]. However, during the manipulation and processing of a microliter-scaled sample, it is often difficult to obtain a representative sample from heterogeneous specimens. Especially, for detection of rare target cells, an enrichment step that increases the effective concentration while reducing the sample volume is required in microdevices [1, 3].

Currently, microfiltration and dielectrophoresis (DEP) have been studied mainly for cell separation and enrichment [1, 4]. Microfilters of tortuous channels [5], comb-shaped filters [6] and weir-type filters [7] have been utilized successfully for the purpose of white blood cell (WBC) isolation from whole blood. However, the microfilters cannot separate typically submicron size pathogenic bacterial cells (0.2 ~ 5 μm) by size exclusion alone since they are much smaller than WBC (6 ~ 20 μm). On the other hand, DEP has been

employed to separate a variety of cells including bacteria [8-11], cancer cells [12-15], stem cells [16, 17], and leukocyte subpopulations [18]. The DEP technique demonstrated ~80% collection efficiency for *E. coli* in deionized water with a flow rate of 400 μL/min [10]. But, its application to whole blood is restricted because it requires a thousand fold dilution to reduce the ionic strength for effective operation [4, 10, 19]. Because of the above limitations, these techniques are difficult to be incorporated into a portable LOC device.

To solve this problem, we have developed a flow-through type microdevice capable of processing large sample volume to capture bacterial cells. To do this, the conditions for bacterial adhesion onto the solid surface were optimized by controlling the surface tension of the chip substrate and the media pH. Based on observed results, pillar arrays were fabricated to increase the surface to volume ratio and enhance bacterial cell adhesion. Our microchip showed outstanding bacterial cell capture efficiency in buffer solution and more importantly even in 50% whole blood. Furthermore, we demonstrated an *in-situ* DNA extraction from captured cells and evaluated the prepared DNA quality in comparison with commercially available Qiagen kit. This novel DNA sample preparation device is a practical approach to be integrated into LOC designed for clinical samples.

2-2. Experimental

2-2-1. Formation of self-assembled monolayer

The glass substrates (25 mm × 75 mm) were cleaned in a piranha solution (a mixture of sulfuric acid (H_2SO_4) and hydrogen peroxide (H_2O_2) for 1 hour and washed with deionized water for 20 minutes. After drying the substrates with nitrogen gas, they were dipped into the prepared coating solution and allowed to react for 1 hour in room temperature. Then, they were twice washed with fresh ethanol for 20 minutes and baked at 110 ℃ for 50 minutes. The coating solution was prepared by dissolving silane compound into ethanol or toluene at a final concentration of 200 mM. The silane compounds, tridecafluorotetrahydrooctyl trimethoxysilane (Gelest) and octadecyldimethyl (3-trimethoxysilyl propyl) ammonium chloride (Gelest) were purchased and used as received. The former was dissolved in toluene and the latter in ethanol. Water contact angle of the substrate was measured with a contact angle meter (Kruss DSA). For the pillar array chips, the prepared coating solution was injected into the fluidic ports by syringe, allowed to react for 1 hour in room temperature, washed with ethanol 3 times, and then dried under vacuum.

2-2-2. Bacteria and culture conditions

Bacterial strains used in this study *Escherichia coli* strain BL21 (*E. coli*), *Staphylococcus epidermis* Evans (American Type Culture Collection No. 12228, FDA strain PCI 1200, *S. epidermis*) and *Streptococcus mutans* Clarke (American Type Culture Collection No. 25175, *S. mutans*) were obtained from Korean Collection for Type

Cultures. *E. coli* and *S. mutans* were grown in 3 mL BHI broth (Brain Heart Infusion, Becton, Dickinson and Company) at 37 ℃ overnight and *S. epidermis* was grown in 3 mL Nutrient broth (Becton, Dickinson and Company) at 37 ℃ overnight.

2-2-3. Cell binding test

E. coli in 100 mM sodium phosphate at pH 4 and 7 was prepared at the final concentration of 1×10^7 cells/mL after twice washing with 1X PBS solution (pH 7.4). A reaction chamber with a volume of 60 μL was constructed by attaching an adhesive plastic patch onto the glass substrate. The surface area used for cell adhesion was 15 mm × 15 mm. After vortexing the cell suspension, a 60 μL aliquot of the suspension was injected into the reaction chamber and allowed to bind to the surface for 5 min at room temperature. After binding, the planar chips were retrieved and washed with the same suspending buffer to remove any weakly adhered bacteria on shaker for 5 min. The adhered bacteria were stained with Gram-staining dye (Becton, Dickinson and Company) for microscopic image analysis. A Keyence VH-Z450 microscope installed with a CCD camera was used for taking photographs of bacteria adhered at three random positions. The number of adhered bacteria per unit area (4800 μm × 4800 μm) was calculated by counting the stained cells in the photograph. A series of pillar arrays with a size of 10 mm × 34 mm were manufactured to have an internal volume of 10 μL as displayed in Table 2-2. The etched chip was anodically bonded with the glass cover with fluidic ports. The

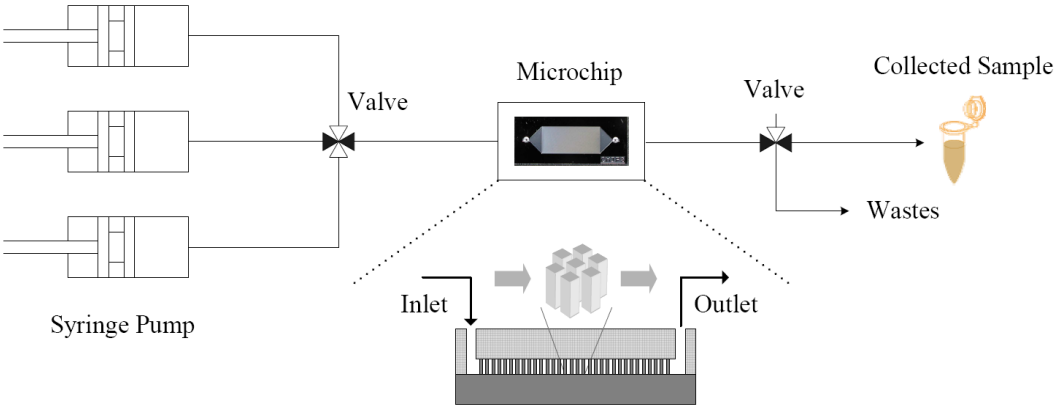

(a)

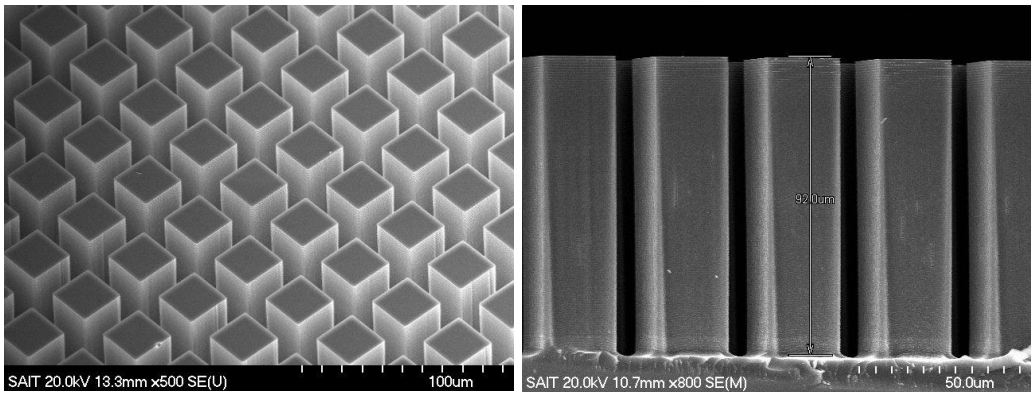

(b)

Figure 2-1. (a) Experimental setup for bacterial DNA sample preparation in a single microchip. (b) SEM image of fabricated pillar arrays used for bacterial DNA preparation from whole blood.

organic self-assembled monolayer was formed on the surface of pillar arrays through the fluidic ports. The microfluidic test module was constructed using a syringe pump (Harvard PHD2000) attached with a custom manufactured jig as illustrated in Figure 2-1a.

2-2-4. Quantification of captured bacteria on surface-modified Si pillar arrays

The initial bacteria suspension was adjusted to an optical density of 0.02 at 600 nm. Cell concentration is approximately $1\sim2 \times 10^7$ cells/mL. Three different concentrations of cells, 10^4 cells/mL, 10^3 cells/mL, and 10^2 cells/mL, were obtained by serial dilution of the initial suspension. 100 μL aliquots of each types of cell suspension were added to 900 μL of 1X PBS buffer (pH 7.4) in a 1.5 mL microcentrifuge tube in triplicate. The recovered solution from the pillar arrays was diluted in a same manner. A 1 mL suspension of each replicate for each concentration was spread on a petridish or Petrifilm (3M). They were incubated at 37 ℃ for 24 hours and colonies formed on the petridish were counted. The number of the initial and recovered bacteria was calculated by multiplying the average number of colonies counted from three replicates by the dilution factor. The number of captured bacteria was determined by subtracting the number of recovered bacteria from the initial amount of bacteria. The capture efficiency was calculated by dividing the number of captured cells by the number of initial cells.

2-2-5. Bacterial DNA preparation from whole blood

A 10^7 cells/mL solution of *E. coli* was spiked into freshly drawn whole blood from a healthy volunteer. In order to decrease the pH level of whole blood (pH 7.2 ~ 7.4) to near pH 4, 100 mM sodium acetate buffer (pH 3) was added to whole blood 1:1 (v/v), which gave a final pH of 5.2. 400 μL of the mixed sample was injected through the surface-modified microdevice with a flow rate of 200 μL/min. After initial loading, the chip was washed with 300 μL of sodium acetate buffer (100 mM, pH 3). For lyzing the captured cells, 5 μL of 0.01 N NaOH was injected and heated up to 95 ℃ for 2 minutes using a heat block with fluidic ports sealed. The extracted DNA was eluted by injecting another 45 μL of 0.01 N NaOH solution and 50 μL of eluted solution was obtained as a result. No further DNA purification steps were followed. As a control experiment, 200 μL of whole blood spiked with *E. coli* was applied to the Qiagen DNA extraction kit (Cat 51304, QIAamp DNA Mini Kit) and 50 μL of purified DNA solution was acquired as described in the Qiagen protocol.

2-2-6. Real-time PCR amplification

Real-time PCR (polymerase chain reaction) assays were performed with a primer set (forward : 5'-YCCAKACTCCTACGGGAGGC-3' and reverse : 5'-GTATTACCGCRRCTGCTGGCAC-3') to amplify a region of 16S ribosomal RNA of the *E. coli* genome using the GenSpector® TMC-1000 instrument (Samsung Advanced Institute of Technology, Korea) [27, 28]. PCR was performed in a silicon-glass-bonded

chip with a total volume of 1 μL reaction mixture containing the Reaction Mix (1b) of 1X LightCycler® FastStart DNA master SYBR Green I (Roche Diagnostics), 250 nM of forward and reverse primers (Bioneer, Republic of Korea), 5 mM $MgCl_2$ (Roche Diagnostics) and PCR grade water (Promega). Taq DNA polymerase (Solgent. Co. Ltd., Republic of Korea) was used to prepare the LightCycler mastermix. After loading, the PCR chip was heated at 95 ℃ for 1 min to denature DNA templates followed by 35 cycles with a denaturation step at 95 ℃ for 5 sec, annealing step at 60 ℃ for 15 sec and extension step at 72 ℃ for 20 sec. After amplification was completed, a melting curve analysis was performed by heating (0.1 ℃/s) the sample from 65 ℃ to 95 ℃. The position of primers is 332F and 536R of 16rRNA gene of the *E.coli* genome and the PCR amplicon was designed to have 204 base pairs. The total time required for the 35 cycles of amplification and the melting curve analysis was 35 min or less. Following PCR, the amplified DNA was quantified using Agilent 2100 Bioanalyzer (Agilent Technologies).

2-3. Results and Discussion

2-3-1. Bacterial cell adhesion

To develop a microdevice for effective capture of bacterial cells, we have searched for an optimal chip surface with high affinity for bacterial cells. It has been reported that two different mechanisms influence the adhesion behavior of bacterial cell on the solid

surface [20-21]. They are the thermodynamic approach associated with surface free energy and electrostatic interaction. However, the thermodynamic approach rather than electrostatic interaction has offered a powerful theoretical tool to predict bacterial adhesion on an inert solid surface [22-24]. Based on these reports, silane materials with different contact angle (surface tension) were coated on planar glass using self - assembled monolayer (SAM). The glass substrate coated with tridecafluorotetrahydrooctyl trimethoxysilane (TDF) and octadecyldimethyl (3-trimethoxysilyl propyl) ammonium chloride (OAC) showed contact angle of 85.7 (±1.7) and 53.7 (±1.2) degrees, respectively, and the non-SAM coated glass had contact angle less than 20 degrees. Three glass substrates for each type were measured.

Their affinities for the bacteria, *E. coli*, at two different pH conditions were measured in a static mode. The pH of suspending buffer was included as an experimental factor because it has been reported that pH can influence the adhesion behavior by either inducing the different hydration level of cell envelope [25] or causing cell precipitation [26]. It was confirmed in our study that pH has a significant effect on cell adhesion in addition to the surface tension as shown in Table 2-1. The highest capture efficiency obtained from TDF surface was estimated to be approximately 1% by a microscopic image analysis. Based on the preliminary results, all subsequent experiments were performed on TDF-coated surface with the pH 4 solution. The low bacteria capture efficiency of the planar substrate may stem from the fact that the accessibility of bacterial cell to solid surface is restricted. Therefore, to maximize the bacteria adhesion, a surface

Table 2-1. Numbers of adhered cells on the SAM-coated planar glass substrate. The media pH and contact angle of the substrate are both significant, p values of all cases are less than 0.05 according to ANOVA (ANalysis Of VAriance) analysis. Three repetitions were performed for each experimental condition and three areas of each substrate were observed for cell counting. Note that the unit is number of cells per unit area (4800 μm × 4800 μm).

	TDF	OAC	Glass
pH 4	54.0 ± 16.7	27.5 ± 4.7	10.0 ± 6.1
pH 7	2.7 ± 3.0	5.2 ± 2.0	6.0 ± 2.3

Table 2-2. Types of pillar arrays and their capture efficiency for *E. coli* cells in 100 mM sodium phosphate buffer at pH 4. Three repetitions were performed.

Chip type	Surface modification	Pillar size (μm^2)	Pillar interspacing (μm)	Surface area increase	Surface to volume ratio (μm^{-1})	Capture efficiency (%)
Chip 1	O	25 × 25	8	8.4	0.226	97.0 ± 2.5
Chip 2	O	50 × 50	17	4.1	0.111	90.1 ± 3.7
Chip 3	O	25 × 25	25	2.5	0.063	91.9 ± 7.1
Chip 4	O	50 × 50	50	1.5	0.037	24.7 ± 4.1
Chip 5	X	25 × 25	8	8.4	0.226	~20
Planar	O	n.a.	n.a.	n.a.	0.004	n.d. (~1)

to volume ratio was increased by replacing planar glass substrate with silicon pillar arrays (Table 2-2).

2-3-2. Bacterial cell capture using surface-modified Si pillar arrays

E. coli cells, at the concentration of 10^7 cells/mL, were chosen as a standard specimen for evaluating the design parameters of pillar arrays (Table 2-2). It was carried out by injecting 200 μL of *E. coli* in sodium phosphate buffer (100 mM, pH 4) through the pillar arrays with a flow rate of 400 μL/min. It was determined that cell capture efficiency of over 90% was achievable with the surface-modified pillar arrays having under 25 μm of pillar interspacing as confirmed by the reduction of colonies grown after passing through the microchips. To confirm the cell adhesion on the solid surface, the lateral sides of pillar posts in the microchip were examined under a microscope after staining the adhered cells with a cell-specific dye and a lot of stained cells were observed on them (data not shown). From these results, it was concluded that *E. coli* cells were retained on the SAM-coated 3-dimensional microstructures. Although Our Chip 1 design gave the best performance due to its highest surface to volume ratio as shown in Table 2-2, Chip 2 was chosen for the further bacterial cell binding tests because it is better suited in terms of pressure drops (data not shown). Binding experiments of *S. epidermis* and *S. mutans* using Chip 2 were conducted and the capture efficiencies of 79% (±11.5) and 76% (±2.7) were obtained, respectively. As a negative control, a non SAM-coated Chip 5 showed only about 20%

efficiency for *E. coli* cells (Table 2-2), suggesting that the controlled surface tension of chip is an essential factor for bacterial cell adhesion.

When the target cells are present in low abundance in clinical samples, the function of enrichment becomes even more important for ensuring the detection sensitivity. The dynamic range for cell capture efficiency was assessed using Chip 2 by varying the initial cell concentrations (Figure 2-2). For *E. coli* cells in the range of 10^3 ~ 10^7 cells/mL, the efficiency was found to be over 70% consistently. It dropped to approximately 38% for 10^9 cells/mL cells, which may exceed the cell binding capacity of the chip.

2-3-3. Bacterial DNA preparation from whole blood

Based on the performance of our microchip in a buffer solution, the bacterial cell capture and its DNA sample preparation process from whole blood were evaluated. We took an approach to extract DNA *in-situ* from the adhered cells on chip surface, because it will simplify the complex DNA preparation steps by implementing the full process from cell capture to DNA isolation in a single microchip. In other words, by lyzing the captured cells instead of releasing them, the developed approach would make it easier to automate DNA preparation procedure efficiently; cell capture from raw sample, washing, lysis and DNA elution. To evaluate the proposed DNA preparation procedure, its performance was compared with a conventional DNA preparation method.

At first, the bacterial cell capture efficiency from whole blood was measured. To do

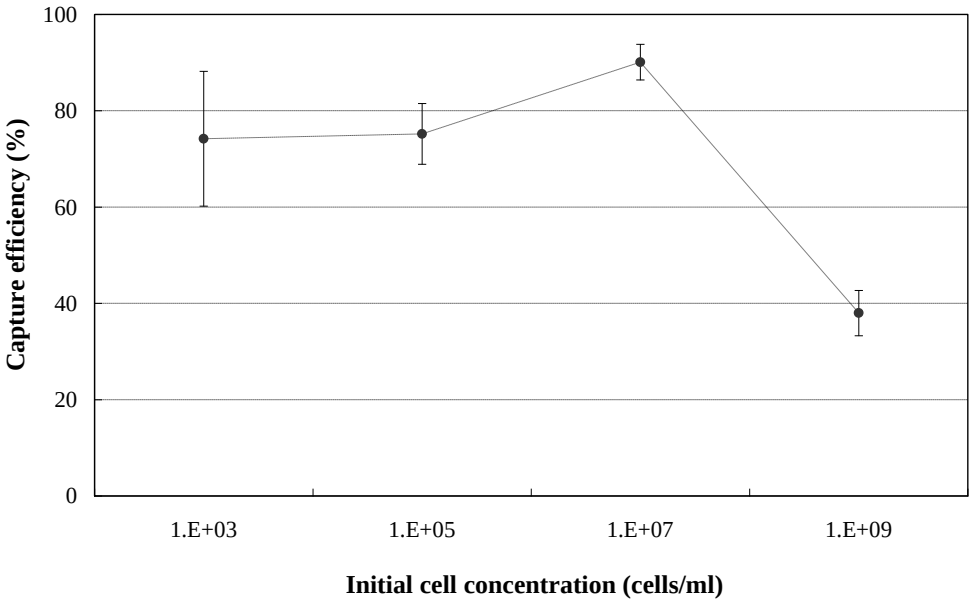

Figure 2-2. Cell capture efficiency with varying initial cell concentrations. Three repetitions were performed.

this, a new chip was fabricated to have a 5 µL of internal volume and size of 10 mm × 23 mm with 12 µm pillar interspacing (pillar size; 25 µm × 25 µm) as displayed in Figure 2-1b. It was found that the *E. coli* capture efficiency was about 40% with 50% whole blood but less than 10% for the unmodified microchip. The presence of other impurities may cause a decrease in capture efficiency compared to that of buffer solution. During the washing step, it was also observed that while the adhered bacterial cells were not released, most of the RBCs, a known PCR inhibitor, were released from the chip. These results indicate that selective collection of bacterial cells and their purification can be achieved before cell lysis step by washing out potential PCR inhibitors.

Next, the quality of bacterial DNA prepared from the proposed procedure was assessed in comparison with the commercial Qiagen DNA preparation kit (Cat 51304, QIAamp DNA Mini Kit). For the accurate comparison of these methods, the total number of *E. coli* injected and final DNA elution volume were controlled to be the same for both methods. The real-time PCR amplification (GenSpector® TMC-1000, Samsung Advanced Institute of Technology) [27, 28] using the eluted DNA from both methods was performed successfully as shown in Figure 2-3. The PCR product was also confirmed and quantified by LabChip® analysis (Agilent Technologies) [29]. It is worthwhile to note that our method yielded almost identical Ct (threshold cycle) value and PCR amplicon concentration when compared to those of Qiagen treated sample (Table 2-3) but the overall process time took less than 10 minutes (Qiagen protocol; 45 minutes). Further, these results prove that our method works very well even without additional DNA

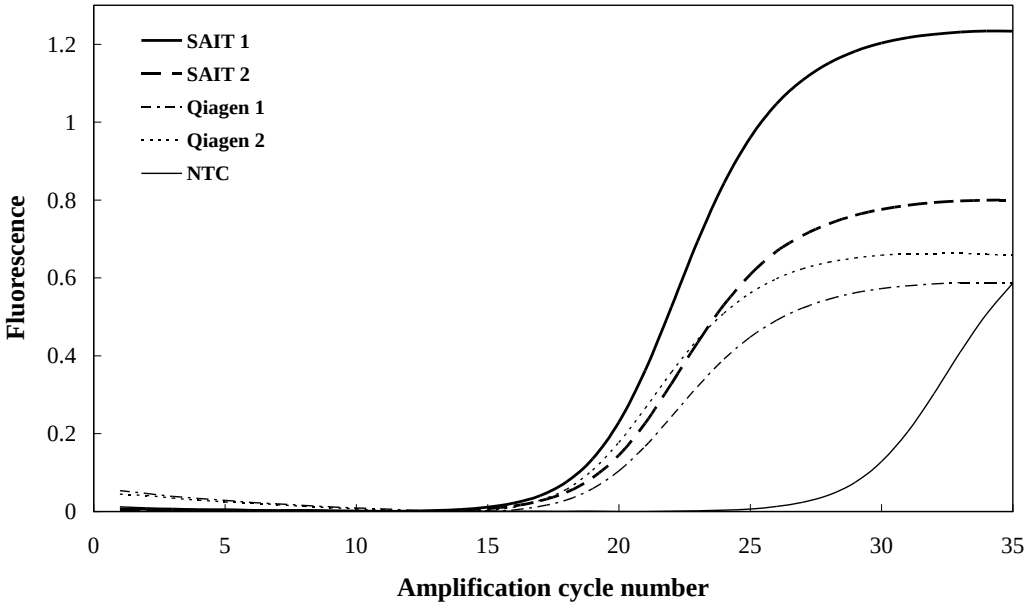

(a)

Figure 2-3a. Real-time PCR amplification using the eluted DNA from surface-modified pillar arrays (SAIT) and its comparison with the commercial Qiagen DNA preparation kit (Qiagen): (a) PCR amplification curve. Two repetitions were performed.

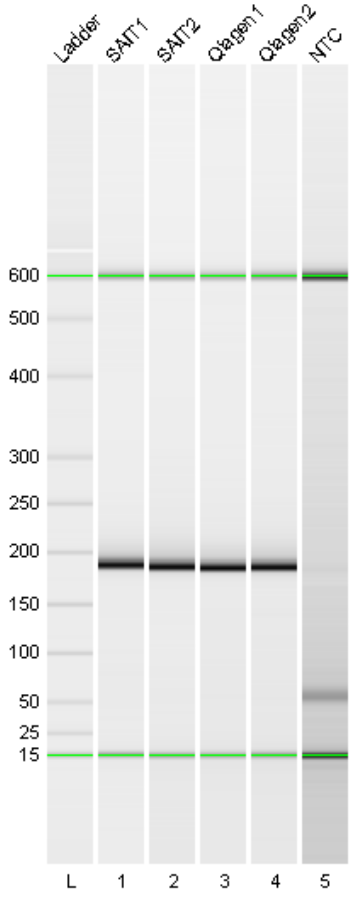

(b)

Figure 2-3b. Real-time PCR amplification using the eluted DNA from surface-modified pillar arrays (SAIT) and its comparison with the commercial Qiagen DNA preparation kit (Qiagen): (b) LabChip® analysis of PCR amplicons. Two repetitions were performed.

Table 2-3. Comparison of Ct value and PCR amplicon concentration obtained from the surface-modified pillar arrays (SAIT) with those from Qiagen kit (Qiagen). Two repetitions were performed.

Sample type	Ct	Concentration (ng/μL)
SAIT 1	18.7	11.8
SAIT 2	18.9	13.1
Qiagen 1	18.4	13.0
Qiagen 2	17.8	11.5
NTC	28.8	-

purification process.

Currently, the recommendation for routine direct-PCR amplification from whole blood is to use less than 1~2% final volume of whole blood in a PCR reaction [30, 31]. Even with the aid of proprietary special PCR facilitators, at most 5~10% of whole blood can be used [32-34]. It has been reported that whole blood is full of PCR inhibitors such as hemoglobin, immunoglobulin G, lactoferrin and serum proteins [31, 35, 36]. While it is helpful to use more blood samples to enhance the sensitivity of PCR, the increased amount of blood increases the PCR failure rate. Therefore, most of the commercial kits require a laborious and tedious process of DNA purification after lyzing the sample [37, 38]. Because of these complex purification steps, the DNA purification process has been difficult to be incorporated into a LOC device. In this regard, our flow-through type device allows even 50% whole blood to be processed which should be translated into an elevated assay sensitivity. The full automation of the developed processes is under development using centrifugal microfluidics based on ferrowax microvalve [39].

2-4. Summary

In this chapter, a novel bacterial DNA sample preparation method using surface-modified pillar arrays has been developed by optimizing media pH and surface tension of chip substrate, which are the main factors for bacterial adhesion onto the solid surface. The fabricated chip showed outstanding bacterial cell capture efficiency not only in buffer

solution but also in 50% whole blood. Furthermore, we have demonstrated that the full process of cell capture to DNA isolation from whole blood can be easily integrated into a single microchip by extracting DNA *in-situ* from captured cells. The prepared DNA quality was found to be good enough for qPCR assay without additional DNA purification steps. We believe that this DNA sample preparation device is well suited to be incorporated into a DNA-based diagnostic LOC system.

References

[1] Huang, Y.; Mather, E. L.; Bell, J. L.; Madou, M. *Anal. Bioanal. Chem.* **2002**, *372*, 49–65.

[2] Lichtenberg, J.; De Rooij, N. F.; Verpoorte, E. *Talanta* **2002**, *56*, 233–266.

[3] Manz, A.; Graber, N.; Widmer, HM. *Sens. Actuators, B* **1990**, *1*, 244-248.

[4] Toner, M.; Irimia, D. *Annu. Rev. Biomed. Eng.* **2005**, *7*, 77-103.

[5] Wilding, P.; Pfahler, J.; Bau, H. H.; Zemel, J. N.; Kricka, LJ. *J. Clin. Chem*. **1994**, *40*, 43–47.

[6] Cheng, JP.; Fortina, S.; Sorrey, LJ.; Wilding, P. *Molec. Diag*. **1996**, *1*, 183–200.

[7] Yuen, PK.; Kricka, LJ.; Fortina, P.; Panaro, NJ.; Sakazume, T.; Wilding, P. *Genome Res*. **2001**, 405–412.

[8] Wang, XB.; Huang, Y.; Hölzel, R.; Burt, JPH.; Pethig, R. *J. Phys. D: Appl.* **1993**, *26*, 1278–1285.

[9] Markx, GH.; Huang, Y.; Zhou, XF.; Pethig, R. *Microbiology* **1994**. *140*, 585–591.

[10] Cheng, J.; Sheldon, EL.; Wu, L.; Heller, MJ.; O'Connell, JP. *Anal. Chem.* **1998**, *70*, 2321–2326.

[11] Huang, Y.; Ewalt, KL.; Tirado, M.; Haigis, R.; Forster, A.; Ackley, D.; Heller, MJ.; O'Connell, JP.; Krihak, M. *Anal. Chem.* **2001**, *73*, 1549–1559.

[12] Becker, FF.; Wang, XB.; Huang, Y.; Pethig, R.; Vykoukal, J.; Gascoyne, PRC. *Proc. Natl. Acad. Sci. USA* **1995**, *92*, 860–864.

[13] Gascoyne, PRC.; Wang, XB.; Huang, Y.; Becker, FF. *IEEE Ind. Appl. Soc. Trans.* **1997**, *33*, 670–678.

[14] Yang, J.; Huang, Y.; Wang, XB.; Becker, FF.; Gascoyne, PRC. *Anal. Chem.* **1999**, *71*, 911–918.

[15] Muller, T.; Schnelle, T.; Gradl, T.; Shirley, SG.; Fuhr, GJ. *J. Liq. Chromatogr. Rel. Technol.* **2000**, *23*, 47–59.

[16] Stephens, MM.; Talary, S.; Pethig, R.; Burnett, K.; Mills, I. *Bone Marrow Transplant* **1996**, *18*, 777–782.

[17] Huang, Y.; Yang, J.; Wang, XB.; Becker, FF.; Gascoyne, PRC. *J. Hematother Stem Cell Res.* **1999**, *8*, 481–190.

[18] Yang, J.; Huang, Y.; Wang, XB.; Becker, FF.; Gascoyne, PRC. *Biophys J.* **2000**, *78*, 2680–2689.

[19] Wang, XB.; Yang, J.; Huang, Y.; Vykoukal, J.; Becker, FF.; Gascoyne, PRC. *Anal. Chem.* **2000**, *72*, 832-839.

[20] Krekeler, C.; Ziehr, H.; Klein, J. *Experientia* **1989**, *45*, 1047-1055.

[21] Bos, R.; van der Mei, H. C.; Busscher, HJ. *FEMS Microbiology Reviews* **1999**, *23*, 179-230.

[22] Absolom, D. R.; Lamberti, F.V.; Policova, Z.; Zingg, W.; van OSS, C. J.; Wilhelm Neumann, A. *Appl. Environ. Microbiol.* **1983**, 90-97.

[23] Busscher, H. J.; Weerkamp, A. H.; van der Mei, H. C.; van Pelt, A. W.; DE Jong, H. P.; Arends, J. *Appl. Environ. Microbiol.* **1984**, 980-983

[24] Prereni, S.I., Zhao, Q., Liu, Y.; Abel, E. *Colloids Surf., B: Biointerfaces* **2006**, *48*, 143-147.

[25] Gaboriaud, F.; Dague, E.; Bailet, S.; Jorand, F.; Duval, J.; Thomas, F. *Colloids Surf., B: Biointerfaces* **2006**, *52*, 108-116.

[26] REEVE; Michael; Alan. **1991**, Patent PCT/GB91/00212; WO 91/12079.

[27] Oh, K. W.; Cho, Y. K.; Kim, J.; Kim, S.; Ock, K. S.; Namkoong, K.; Yoo, K.; Park, C.; Lee, Y.; Kim, Y. A.; Han, J.; Lim, H.; Kim, J.; Yoon, D.; Lim, G.; Kim, S.; Hwang, J. J.; Pak, Y. E. In preceedings *Micro Total Analysis System 2004*, Malmo, **2004**, 150–152.

[28] Cho, Y. K.; Kim, J.; Lee, Y.; Kim, Y. A.; Namkoong, K.; Lim, H.; Oh, K. W.; Kim, S.; Han, J.; Park, C.; Pak, Y. E.; Ki, C. S.; Choi, J. R.; Myeong, H. K.; Ko, C. *Biosens. Bioelectron.* **2006**, *21*, 2161-2169.

[29] The PCR amplicon was designed to have 204 base pairs. Considering DNA 500 LabChip® Kit (Caliper Life Sciences) used with Agilent 2100 Bioanalyzer (Agilent Technologies) has the sizing accuracy of 10% (CV), it is reasonable that the bands around

190 bp in Figure 2-3b are those of PCR amplicons.

[30] Wilson, I. G. *Appl. Environ. Microbiol.* **1997**, *63*, 3741-3751.

[31] Mercier, B.; Gaucher, C.; Feugeas, O.; Manzurier, C. *Nucleic Acids Res.* **1990**, *18*, 5908.

[32] http://www.bioventures.com, GeneReleaser®.

[33] http://www.shimadzu.com, Ampdirect®.

[34] http://www.piercenet.com, Lyse-N-Go® PCR Reagent.

[35] Abu Al-Soud, W.; Radstrom, P. *J. Clin. Microbiol.* **2001**, *39*, 485-493.

[36] Abu Al-Soud, W.; Jonsson, L. J.; Radstrom, P. *J. Clin. Microbiol.* **2000**, *38*, 345-350.

[37] http://www.qiagen.com.

[38] http://www.molzym.com.

[39] Park, J. M.; Cho, Y. K.; Lee, B. S., Lee, J. G.; Ko, C. *Lab Chip* **2007**, *7*, 557-564.

Chapter 3. Fabrication of low-cost polymer micropillar arrays for on-chip extraction of bacterial DNA

3-1. Introduction

Nucleic acid-based micro total analysis system (μTAS) is a promising approach to fully automate the analytical procedures on a microchip platform. In particular, incorporation of target sample preparation, amplification and detection into a miniaturized lab-on-a-chip format has the potential to revolutionize many life science applications and related areas, including clinical diagnoses, biological and forensic analyses. These sample-in-answer-out devices can offer many advantages, such as low consumption of reagent, rapid analysis, easy operation, and improved reproducibility [1-4].

In contrast to protein analysis, an extraction or purification step to acquire DNA of interest from desired cells is a prerequisite for successful genetic analysis [5-9]. Most conventional bench-top DNA purification techniques are difficult to be used in microchips since these often require centrifugation or other hands-on processing steps. To address these challenges, a large number of solid phase extraction techniques, which can be integrated into microfluidic devices, have been developed [4, 10]. In spite of the aforementioned benefits associated with the decreased cost through miniaturization, most

of published works on DNA extraction have been predominantly performed with expensive inorganic substrates, such as silicon, glass, quartz because of their superior material properties and easy adaptation to well-established MEMS fabrication techniques [4, 7]. However, there are some potential drawbacks with the inorganic-based microdevices. The cost for materials and fabrication processes such as photolithography, etching (dry and wet) and high temperature bonding is high [2, 4, 10], which have been often ignored in the research stages of microfluidic devices. Therefore, it is potentially beneficial to develop fabrication technologies that allow production of such devices at a cost comparable to that of the conventional bench-top devices. In this regard, polymer microdevices, which can be manufactured through relatively low cost processes such as injection molding or hot embossing, are an attractive solution to alleviate the above-mentioned cost issues [2, 10-13]. Nonetheless, transition from inorganic to organic materials is not trivial, for which several challenges need to be suitably addressed including fabrication of large surface area (high surface-to-volume ratio microstructures) for effective biomolecule manipulation [4, 10, 14] and chemical compatibility of polymer during biochemical assays [11-12]. A handful of studies have been reported on DNA extraction with plastic microfluidic devices. In order to generate large surface area, most of the previous studies employed installation of silica-based matrix, such as packed bead, sol-gel and bead-polymer monolith, on a chip scale after fabrication of polymeric microchamber [15-18]. In addition, micropost-anchored carboxyl groups on polycarbonate substrate exhibited DNA purification capability with the aid of

polyethylene glycol (PEG) solution and ethanol [19-20].

Until now, chaotrope-based DNA purification method has become widely accepted in miniaturized devices because chaotropes (*e.g.* guanidinium thiocynate) have an ability to disrupt cell membrane as well as to bind DNA onto a solid surface (*i.e.* silica), which eliminates additional need for chamber or buffer change [4, 9, 15-18]. However, it is desirable to avoid the use of such chemicals including chaotropes or organic solvent (*e.g.* ethanol) within microfluidic environments as they are well-known PCR inhibitors [10]. They have been usually applied to bench-top processes involving centrifugation steps. Therefore, a different DNA extraction scheme that would be more compatible with downstream processes (*e.g.*, electrostatic interaction [21-22] and filtration [23]) is still needed.

Our interest here lies in fabricating a low-cost polymeric microchip that has bacterial DNA extraction capability comparable to inorganic-based microchips and that can perform full pre-PCR processes from bacterial cell capture to DNA isolation. It was previously reported that bacterial DNA preparation can be done on microchips with surface-modified Si micropillars [24-25]. Bacterial cells can be selectively captured on them from buffer suspension or whole blood by optimizing surface tension of solid substrate and media pH based on bacterial adhesion thermodynamics [26]. Furthermore, it doesn't require the PCR-inhibitory purification chemicals such as chaotropes, PEG, and organic solvent. According to the thermodynamic adhesion model, decreasing surface tension of the solid substrate (*i.e.* increasing hydrophobicity) will lead to higher cell

adhesion when surface tension of buffer solution (*ca.* 73 erg/cm^2) is higher than that of bacterial cell (*ca.* 66 ~ 69 erg/cm^2) [26]. Organosilane containing functional groups reactive to SiO_2 surface was chosen for controlling surface tension of the solid substrate in our previous report [24]. While performance of this approach was found to be equivalent to that of a commercial DNA extraction kit, the microchip was produced from expensive glass and silicon substrates using conventional photolithography processes including patterning, deep reactive-ion-etching and high temperature anodic bonding.

In this work, we have developed a fabrication method to replace inorganic substrates with much cheaper polymer materials. Micropillar arrays on polymethylmethacrylate (PMMA) substrate were generated by hot embossing technique with an electroformed Ni mold, and organosilane was coated following room temperature deposition of SiO_2. Finally, the processed PMMA substrate was bonded to polydimethylsiloxane (PDMS) sheet to enclose the microchannels. PDMS is a well-known polymeric material that has been widely used in various microfluidic devices. In particular, bonding characteristic of PDMS to a variety of hydrophilic inorganic oxide materials such as SiO_2 are attractive in that only surface activation is required without the use of adhesives or solvents. To facilitate PDMS-interface bonding to organosilane-modified SiO_2 surface, photocatalyst was employed to selectively remove a thin organosilane film on top plane of the micropillars without any adverse effects on their lateral surface. This approach allowed us to fabricate a low-cost plastic microchip without loss of bioanalytical activities such as bacterial cell capture and PCR compatibility.

3-2. Experimental

3-2-1. Organosilane-coated glass/Si microchip fabrication

The glass/Si microchip was fabricated using standard MEMS techniques. First, a 6-inch silicon wafer was spin-coated with positive photoresist (AZ GXR 601, Clariant, Switzerland) and patterned using an EV620 mask aligner (EV Group, Austria). The patterned photoresist was developed, and the wafer was dry-etched to 50 μm with inductively coupled plasma (ICP) in a Deep Reactive Ion Etching (DRIE) etcher (STS, UK). The microchip (23 mm × 10 mm) was designed with an internal volume of 5 μL and a micropillar interspacing of 12 μm, and size of each micropillar was 23 μm × 23 μm × 50 μm. Then, 5000 Å of silicon dioxide was grown on the Si wafer and anodically bonded to a glass wafer with inlet and outlet holes formed through a sandblast technique. In order to modify the micropillar surfaces, an organosilane solution containing 200 mM of tridecafluoro-1,1,2,2-tetrahydrooctyl trimethoxysilane (Gelest, USA) in toluene was injected into fluidic ports with a syringe. After allowing the reaction for 1 hr, the micropillar surfaces were washed with fresh ethanol three times, and then dried at 110 ℃ for 50 min.

3-2-2. Ni mold fabrication and hot embossing

In order to fabricate PMMA pillar arrays, additional steps, such as Ni electroplating for mold, hot embossing, and SiO_2 evaporation, were processed over the Si pillar arrays. For efficient embossing process, nanoscallops on the lateral surfaces of the Si micropillars formed during the Bosch process were removed through wet oxidation (8000-Å-thick SiO_2 layer) and etching with hydrofluoric acid solution. Chromium (1000 Å) and copper (1000 Å) were sequentially deposited onto the etched silicon surface with a sputtering system (Atech, Korea). Cr/Cu served as a conducting seed layer for electroforming in the next step. The Cr/Cu layer was connected to a negative electrode and electroplated in a nickel solution-based sulfamic acid with current density of 20 mA/cm^2 at 55 ℃ for 20 hr. Finally, silicon was etched for 8 hr at 85 ℃ in 25 wt% potassium hydroxide solution to generate Ni mold.

The hot embossing technique (HEX03, Jenoptics, Germany) was applied to construct the micropillar arrays in PMMA sheet (Rohm, Germany). During the process, the PMMA sheet was sandwiched between a flat plate and the fabricated Ni mold. While heating the PMMA sheet at 150 ℃, an embossing force (35 kN) was applied for 800 sec. The mold was subsequently cooled to 26 ℃ with the force maintained to preserve the microstructures, and then demolding was performed. Afterwards, Cr (200 Å) was sputtered, and SiO_2 (5000 Å) was successively deposited on the replicated PMMA sheet through e-beam evaporation (Korea Vacuum, Korea) at room temperature. Finally, the organosilane layer (tridecafluoro-1,1,2,2-tetrahydrooctyl trimethoxysilane) was coated on the deposited SiO_2 layer at the wafer level.

3-2-3. PDMS-interface bonding with TiO_2/UV treatment

TiO_2 sol solution was prepared by mixing 6 mL of titanium (IV) isopropoxide ($Ti\{OCH(CH_3)_2\}_4$, Sigma-Aldrich, USA) and 0.8 mL of 0.1 N HCl in isopropanol (85 mL). The mixed solution was mildly stirred to form TiO_2 sol overnight and was spin-coated onto a transparent Pyrex wafer with 0.5 mm-thickness (Corning, USA) at the speed of 4000 rpm for 40 sec. The processed glass wafer was calcined (500 ℃, 1 hr) in a furnace, and the measured thickness of TiO_2 was *ca.* 400 Å. The organosilane-coated pillar arrays (Si or PMMA) were irradiated for 10 min using TiO_2/Pyrex as a photomask with an UV aligner (Shinu, Korea) at the wafer level. O_2 plasma treatment of PDMS sheet with thickness of 0.7 mm (HT-6200, Rogers, USA) was performed in a plasma cleaner (Harrick, USA) for surface activation. It was subsequently bonded to TiO_2/UV-treated surface-modified Si or PMMA pillar arrays.

3-3. Results and Discussion

3-3-1. PDMS bonding to organosilane-coated micropillar arrays

Sealing of open microfluidic components is the last step to produce enclosed fluidic environments and thus, bonding is one of the major concerns in most thermoplastic fabrication processes. The versatile use of polymer materials has enabled a number of

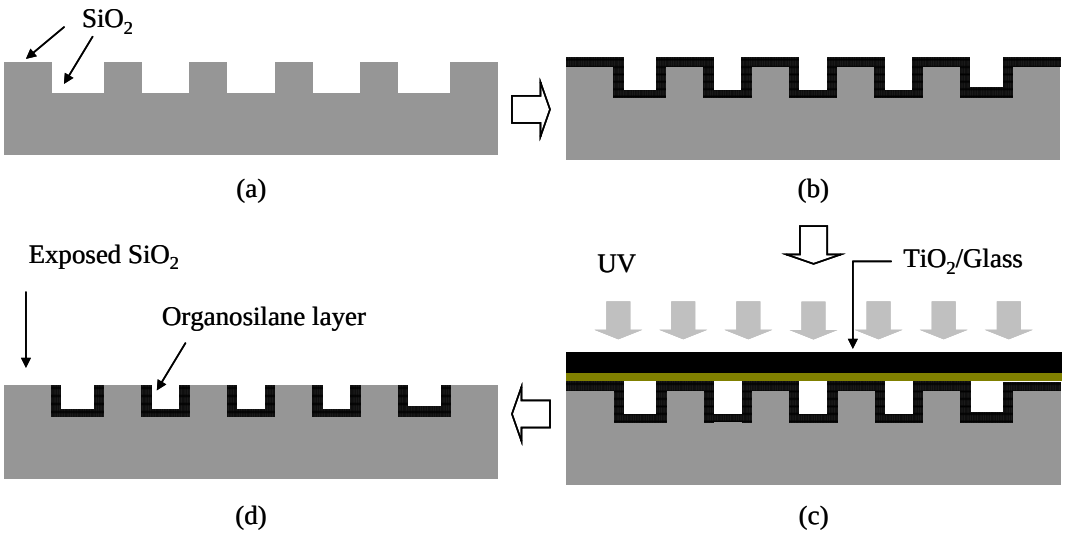

Figure 3-1. Scheme for selective removal of the organosilane layer using photocatalyst/UV: (a) Pillar arrays; (b) Organosilane wet coating; (c) Transparent photocatalyst-containing layer (TiO_2/Glass) in contact with the top plane of the micropillars during UV irradiation; (d) Selective removal of organosilane on the top plane of the micropillars (exposed SiO_2) - Ready for bonding with PDMS.

bonding techniques on the basis of adhesive, thermal, solvent and surface modification [14]. Depending on the functional requirements of the final microfluidic system, several considerations must be taken into account when choosing an appropriate sealing technique. These include bond strength and interfacial properties that are associated with solvent compatibility, surface chemistry, and optical properties [14]. Furthermore, the device functionality should be intact while performing the given bonding process. For example, the presence of ultra-thin organosilane (tridecafluoro-1,1,2,2-tetrahydrooctyl trimethoxysilane) film, which is an indispensable element for bacterial cell capture [24], restricts direct application of most conventional thermoplastic bonding techniques (*i.e.* adhesive, solvent, thermal bonding) because they can deteriorate integrity of organosilane and therefore lead to negative bioanalytical activities in terms of bacterial cell capture efficiency and PCR compatibility. Moreover, the existence of inorganic (SiO_2)-organic (PMMA) interface on the micropillars of the bottom PMMA substrate sets a limit on the bonding temperature around room temperature since an excessive thermal energy can destroy structural integrity due to different thermal expansion coefficients [28].

To overcome some of the above limitations, PDMS-interface bonding technique based on surface activation can be an attractive alternative since it can not only be processed at room temperature but also provide good bond strength over *ca.* 300 kPa [29] without any adhesive, solvent, and thermal treatment. In addition, it can make selective contact with the top surface, which serves as the bonding region, while protecting the lateral wall of the micropillars responsible for bioanalytical activity throughout the

processes. Direct PDMS bonding to the organosilane-modified solid surface, however, is still difficult since permanent siloxane bonds (Si-O-Si) cannot be formed between the mating surfaces [30], even if the PDMS sheet were activated by plasma. Therefore, the organic layer on the top plane of the micropillars must be selectively removed without affecting the film on the lateral surface of the micropillars. To this end, nonselective conventional surface activation methods, such as plasma or UV/O_3 treatment, are not suitable. While welding through the use of ultrasonic energy has been shown to achieve local bonding, it requires a special chip design to effectively direct and focus energy at the desired welding points [31-32].

To enable localized PDMS bonding onto the micropillars, photocatalyst was introduced here to remove the organic layer selectively on the mating surface and to regenerate silanol groups (Si-OH) (Figure 3-1). The photocatalyst activated by UV irradiation generates active ions (*e.g.*, hydroxyl radicals ($OH^{\bullet}$) and superoxide (O_2^-)), which can decompose the organic film in contact with the photocatalyst. Particularly, hydroxyl radicals are strong oxidizers (second only to fluorine) and thus are highly reactive, capable of completely oxidizing organic species [33]. Also, photocatalytic oxidation was successfully utilized to pattern the organosilane layer on planar solid substrates through selective degradation [34]. Decomposition of the organic layer following TiO_2/UV irradiation (24 mW/cm^2, 10 min) was observed through drastic reduction of water contact angle from *ca.* 80 to *ca.* 5 degrees as shown in Figure 3-2. Based on these results, it was expected that the increased surface energy as a result of the

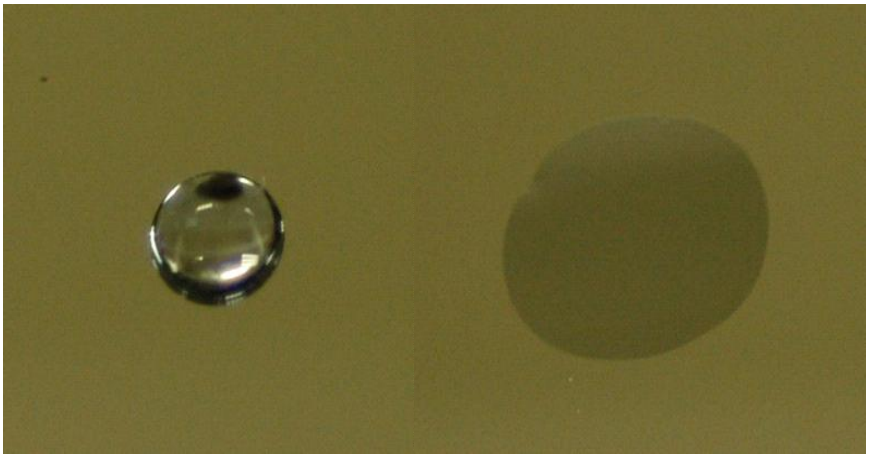

Figure 3-2. Decomposition of the organosilane layer on Si wafer using photocatalytic oxidation. The Si wafer was coated with organosilane, and then exposed to UV irradiation under TiO_2/Glass layer (5 min). The water contact angle was *ca.* 80 degrees before organosilane removal (left-hand side) and less than 5 degrees afterwards (right-hand side).

exposure of SiO_2 surface would contribute to bonding between the micropillars and the surface-activated PDMS sheet.

3-3-2. Fabrication of the PDMS/Si microchip using photocatalyst

First, we attempted to substitute the top glass substrate of the Glass/Si chip with the PDMS sheet. In order to prevent destruction of the organosilane layer during the high temperature anodic bonding of glass and Si (< 600 ℃), the organosilane layer had to be coated chip by chip after the bonding process. However, considering the manufacturing throughput and process integration, it was highly desirable to coat organosilane on the micropillar surface at the wafer level before the bonding process. This was achieved by utilizing the room temperature PDMS-interface bonding technique coupled with TiO_2/UV treatment. The fabricated PDMS/Si chip was evaluated by comparing its bacterial cell capture efficiency and quantitative PCR results to those of Glass/Si chip. Bacterial cell capture, wash, *in-situ* lysis and DNA elution were sequentially performed [24]. During the bacterial DNA extraction process, neither chaotropes nor organic solvents were used. For microchips not treated with the photocatalyst, leakage was observed while flowing the liquid sample, and further tests were abandoned (data not shown). Quality of the bacterial DNA extracted from both chips was assessed by performing real-time PCR amplification [27].

Incomplete bonding or deterioration of the organosilane film on the lateral surface

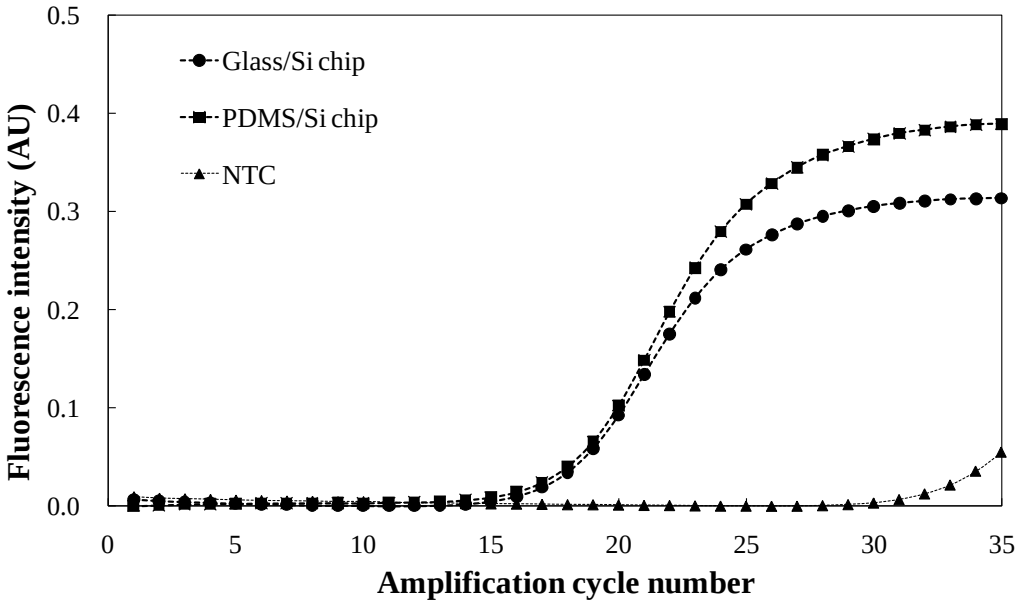

Figure 3-3. Real-time PCR amplification of the extracted DNA from the PDMS/Si and the Glass/Si chips (TMC-1000 PCR machine). Three repetitions were performed, and a representative example is displayed. NTC is a negative control sample.

would negatively affect bacterial capture efficiency and C_T (threshold cycle) values of real-time PCR amplification since probability of bacterial adhesion onto the lateral surface of the micropillars or bacterial affinity would be reduced [24]. Both chips showed over 90% *E. coli* capture efficiencies and similar C_T values (18.9 ± 0.10 for the PDMS/Si chip and 18.7 ± 0.22 for the Glass/Si chip) as displayed in Figure 3-3. These results suggest that the photocatalytic selective oxidation is an effective method for localized bonding of PDMS to organosilane-modified surface. In addition, any notable PCR inhibition from PDMS material was not detected. The proposed aqueous extraction technique may yield lower DNA purity compared to other conventional methods (*e.g.*, chaotropes) due to the presence of cell membrane impurities. Nevertheless, it has some advantages including the rapid process time, simplicity, no need for PCR-inhibitory purification reagents (*e.g.*, chaotropes, PEG, and organic solvents), and therefore integration into microchips. Moreover, the negative effects of the cell membrane impurities on the real-time PCR amplification (Ct value and target amplicon production) were found to be negligible (data not shown).

3-3-3. Polymer substrate imprinting

Hot embossing technique is the most widely used replication process to fabricate plastic microstructures for microfluidic applications. In addition, it is a cost-effective method that can replace silicon DRIE process to generate high surface-to-volume ratio

microstructures. Among a variety of thermoplastic materials, PMMA was chosen as a polymer substrate for the micropillar arrays since it is optically transparent and easily processable like polycarbonate [11-12]. In fact, we have tested PDMS, polycarbonate, polyethylene, and PMMA for the bottom plates. Although it was easy to fabricate the micropillar arrays using PDMS, modification of the PDMS surface was quite challenging. Compatibility with organic solvent had to be taken into account. Solvent-induced PDMS swelling could inhibit surface modification with organosilane, damage structural integrity, and generate PCR-inhibitory chemicals. In order to avoid such problems, we attempted to passivate the PDMS surface by depositing SiO_2 layer where alkoxy groups of the organosilane could hydrolyze and condense. However, interface between the flexible PDMS and SiO_2 layer was found to be very unstable even in the presence of an adhesion promoter and significant amount of crack was observed. In contrast, such behaviors were not observed with PMMA. Moreover, PMMA showed the best pattern qualities over polyethylene and polycarbonate during optimization of the hot embossing processes. Nickel mold, the most suitable master for high-volume replication, was fabricated by electroplating the silicon microstructures (Figure 3-4a) [35]. Imprinting processes were optimized with particular focus on minimizing accumulation of substrate material on top edge of the micropillar sidewall. This artifact appears when the mold pulls up the interacting substrate material during demolding step. Uniformity of the top surface led to conformal contact, thereby allowing tight seal of all micropillars between the two substrates. After optimizing the embossing conditions including heating temperature,

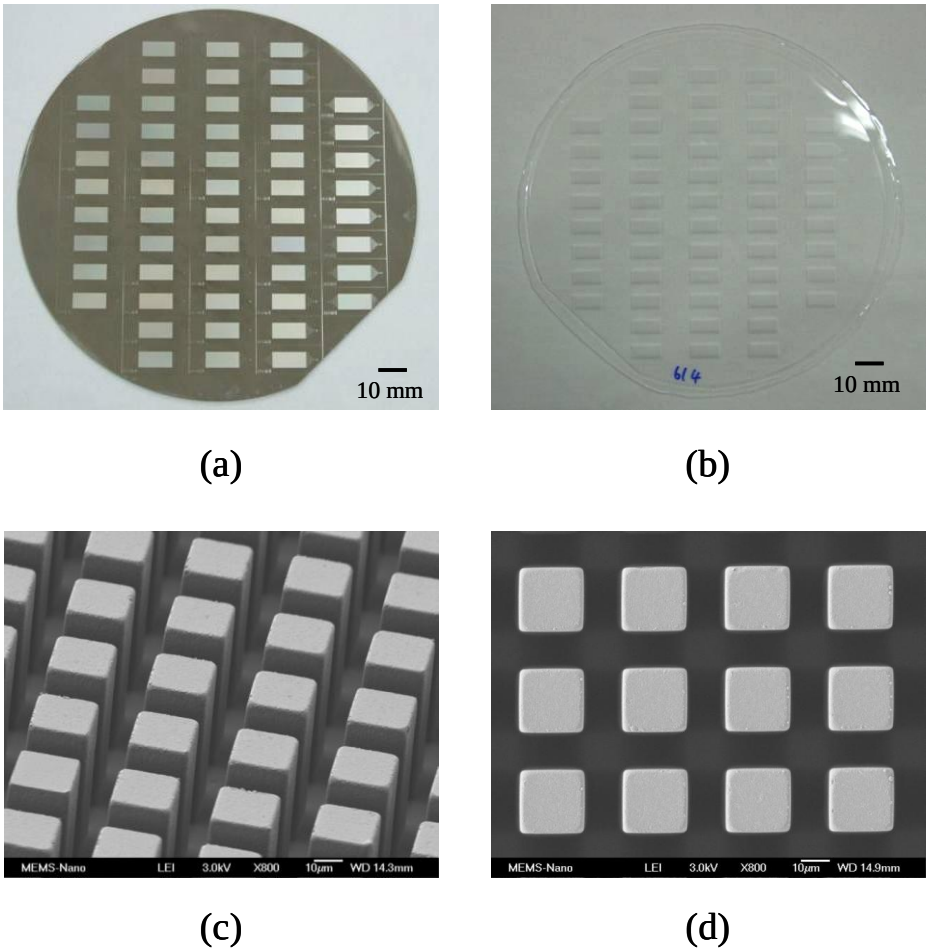

Figure 3-4. Pictures of the fabricated 6-inch Ni mold (a) and corresponding embossed PMMA sheet (b). SEM images of the replicated PMMA micropillar arrays. Each micropillar possessed the size of 23 μm × 23 μm × 50 μm with interspacing of 12 μm (c & d).

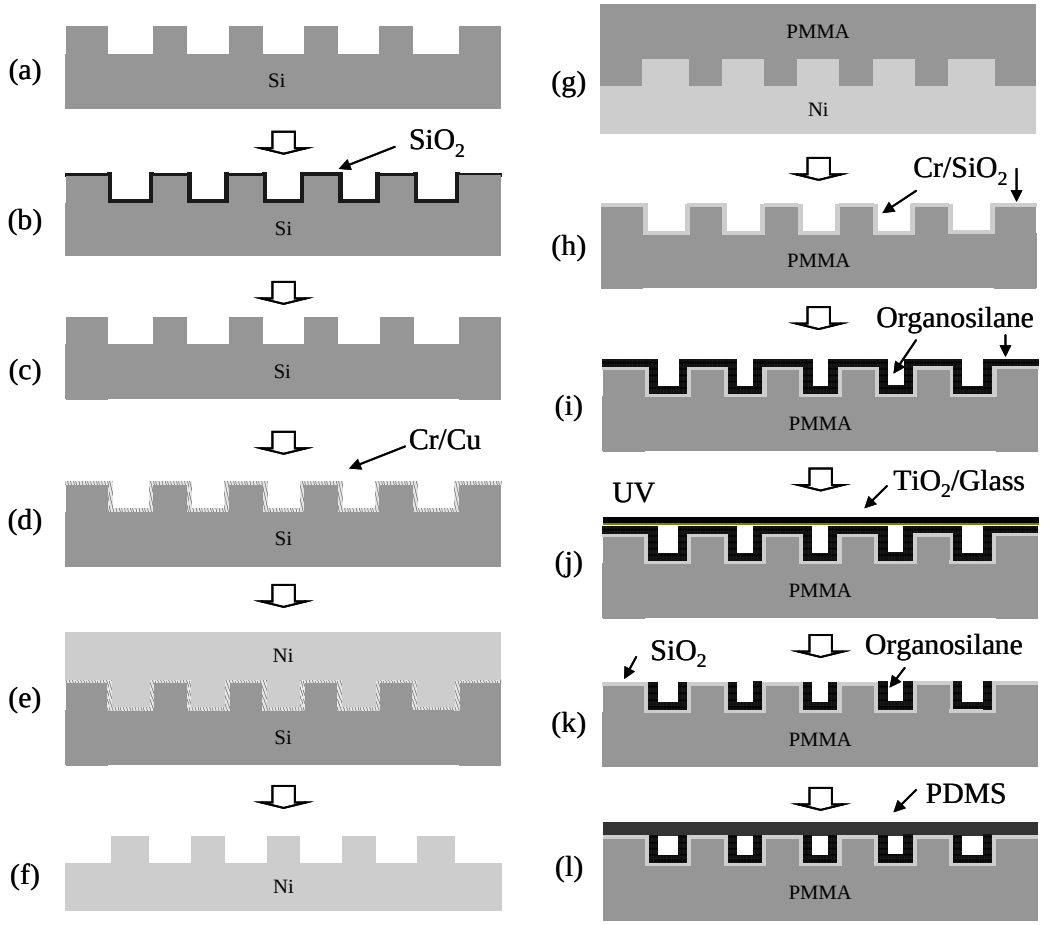

Figure 3-5. Fabrication scheme of the PDMS/PMMA chip: (a) Si pillar arrays; (b) Oxidation for nanoscallop removal; (c) SiO_2 removal; (d) Cr/Cu deposition; (e) electroforming; (f) Si wet etching and resulting Ni mold; (g) PMMA replication; (h) Cr/SiO_2 deposition; (i) Organosilane wet coating; (j) TiO_2/UV treatment; (k) Selective removal of organosilane; (l) Bonding with O_2 plasma-treated PDMS.

force, and time on the hot embossing system, well-defined micropillars were formed as shown in Figure 3-4. Pattern deformation was rarely observed, and the target features had the size of 23 μm × 23 μm × 50 μm with interspacing of 12 μm, which were faithfully replicated on the PMMA substrate. Furthermore, the top plane of the micropillars was flat (RMS roughness of *ca.* 55 nm), which would enable tight bonding to the PDMS sheet in subsequent steps.

3-3-4. Fabrication of the PDMS/PMMA microchip using photocatalyst

Next, we attempted to replace the bottom Si substrate with the embossed PMMA sheet. Because PMMA does not possess functional groups to react with organosilane, SiO_2 was deposited using e-beam evaporation at room temperature after considering different thermal expansion behavior of SiO_2 and PMMA. Figure 3-5 summarizes full fabrication process of the PDMS/PMMA polymer microchip.

The manufactured PDMS/PMMA chip was evaluated by conducting bacterial DNA extraction from urine samples in comparison to the Glass/Si chip. To mimic infectious disease conditions caused by pathogens in urine samples, such as urinary tract infection or sexually-transmitted disease, *E. coli* was spiked into freshly drawn urine from volunteers. The PDMS/PMMA chips showed similar capture efficiency of 48 ± 10% compared to that of 52 ± 4% from the Glass/Si chip. Also, similar Ct values (17.0 ± 0.26 for the PDMS/PMMA chip and 16.6 ± 0.08 for the Glass/Si chip) were obtained, and

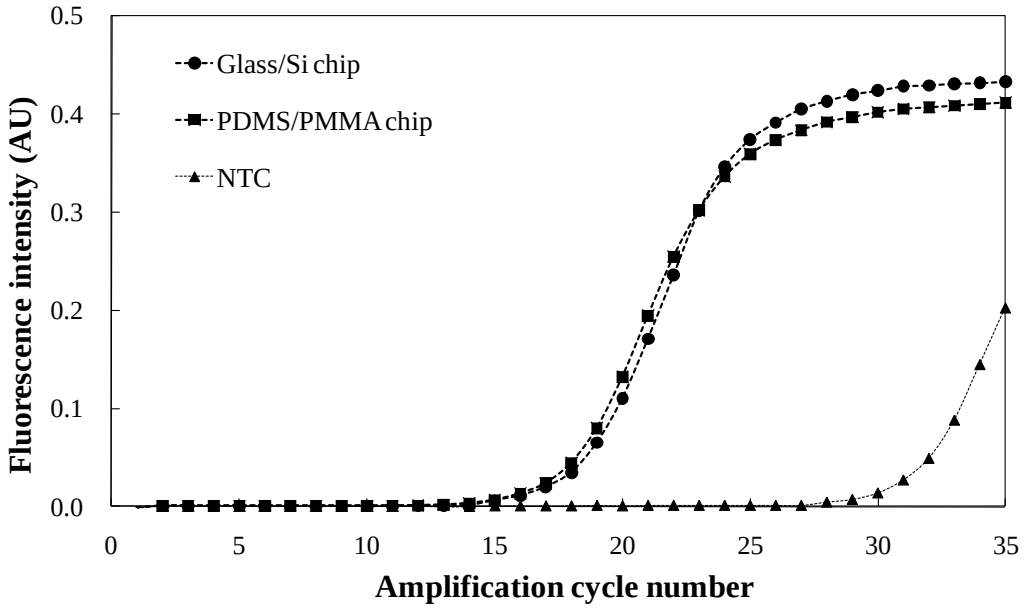

Figure 3-6. Real-time PCR amplification using the extracted DNA from the PDMS/PMMA and the Glass/Si microchips (TMC-1000 PCR machine). Three repetitions were performed, and a representative example is displayed. NTC is a negative control sample.

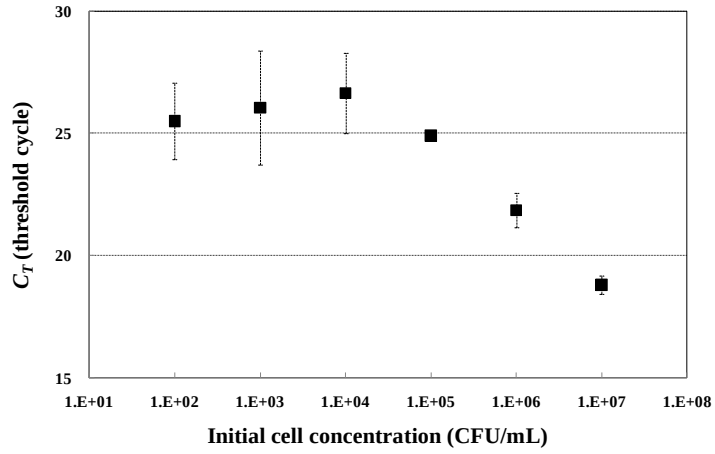

(a)

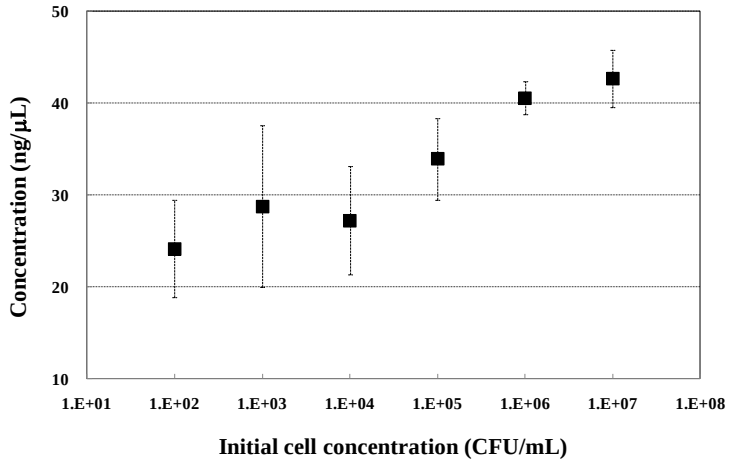

(b)

Figure 3-7. Ct values (a) and amplicon concentration (b) as a function of initial cell concentration with the PDMS/PMMA microchips. Three repetitions were performed for each cell concentration.

PCR inhibition from polymer materials was not observed (Figure 3-6). These results indicate that the low-cost polymeric microdevice presented here can replace current silicon-based microchips. However, the PDMS/PMMA microchip resulted in larger standard deviation values in capture efficiency and Ct than those of the PDMS/Si and Glass/Si microchips. One potential explanation is that the micropillars were not completely bonded to PDMS because the embossing process could have generated uneven top surface on some of the micropillars. Further optimization of the embossing process to improve the micropillar qualities is under investigation.

In order to further characterize the fabricated microchip, we measured its cell binding capacity and limit of detection (LOD). We applied various concentrations of *E. coli* (*i.e.*, 10^3, 10^4, 10^5, 10^6, 10^7, 10^8, and 10^9 CFU/mL) in acetate buffer (pH 4). When 200 μL of each sample was injected to the microchip, capture efficiency over 90% was maintained in the range between 10^3 CFU/mL and 10^8 CFU/mL. However, it was dramatically reduced to ~ 40% for the 10^9 CFU/mL sample. Therefore, it can be speculated that the present microchip has cell binding capacity over ~ 10^7 (0.2×10^8) CFU of *E.coli*. To determine LOD, different cell concentrations of *E.coli* (10^7, 10^6, 10^5, 10^4, 10^3, 10^2 and 0 CFU/mL) in acetate buffer (pH 3) were spiked into urine samples at 1:1 (v/v) ratio, and DNA extraction was performed. It was possible to detect 10^2 CFU/mL of *E. coli* in the urine samples through the present method (Figure 3-7a). Although quantitative increase of the Ct values was not observed with the samples with *E.coli* concentration from 10^5 CFU/mL to 10^2 CFU/mL, production of target amplicon (204 bps) was confirmed through

melting curve analysis, and its concentration was quantified by gel-electrophoresis as shown in Figure 3-7b. It may stem from the intercalating properties of SYBR Green dye which binds the non-specific products such as dimmers or primers [36]. The negative control samples yielded the Ct of 33 and *ca.* 7.1 ng/μL of amplicon concentration, which may originate from the normal flora in urine.

3-4. Summary

In this chapter, we have developed a low-cost polymeric microfluidic device to extract DNA from bacterial cells for molecular diagnostics. In order to replace conventional Glass/Si microchips with a polymer-based microchip, hot embossing using Ni mold to generate micropillar arrays, organosilane coating, and room temperature PDMS-interface bonding to the organosilane-modified surface were performed. After modification of PMMA micropillar surface with organosilane for bacterial cell capture, the microchip was tightly sealed with plasma-treated PDMS sheet through photocatalytic oxidation based on TiO_2/UV treatment. The photocatalyst selectively decomposed the thin organosilane film on the bonding region without adverse effects on the bioanalytical performance including bacterial cell capture efficiency and PCR compatibility. Using the constructed PDMS/PMMA microchip, capture efficiency of 48 ± 10% and detection limit of 10^2 CFU/mL were achieved from 2-fold diluted urine samples, which were comparable to those of Glass/Si microchips. In addition, any notable PCR inhibition from the polymer

materials was not observed. Furthermore, the proposed bonding method allowed us to fabricate the PDMS/PMMA microchip at the 6-inch wafer level with direct application to on-chip extraction of bacterial DNA.

References

[1] Chen, L.; Manz, A. ; Day, P. J. R. *Lab Chip* **2007**, *7*, 1413-1423.

[2] Chin, C. D. ; Linder, V. ; Sia, S. K. *Lab Chip* **2007**, *7*, 41-57.

[3] Manz, A.; Graber, N.; Widmer, HM. *Sens. Actuators, B* **1990**, *1*, 244-248.

[4] Wen, J.; Lgendre, L. A.; Benvenue, J. M. ; Landers, J. P. *Anal. Chem.* **2008**, *80*, 6472-6279.

[5] Abu Al-Soud, W.; Jonsson, L. J.; Radstrom, P. *J. Clin. Microbiol.* **2000**, *38*, 345-350.

[6] Abu Al-Soud, W.; Radstrom, P. *J. Clin. Microbiol.* **2001**, *39*, 485-493.

[7] Huang, Y.; Mather, E. L.; Bell, J. L.; Madou, M. *Anal. Bioanal. Chem.* **2002**, *372*, 49–65.

[8] Lichtenberg, J.; De Rooij, N. F.; Verpoorte, E. *Talanta* **2002**, *56*, 233–266.

[9] Price, C. W.; Leslie, D. C.; Landers, J. P. *Lab Chip* **2009**, *9*, 2484-2494.

[9] Wilson, I. G. *Appl. Environ. Microbiol.* **1997**, *63*, 3741-3751.

[11] Becker, H.; Gartner, C. *Electrophoresis* **2000**, *21*, 12-26.

[12] Becker, H.; Gartner, C. *Anal. Bioanal. Chem.* **2008**, *390*, 89-111.

[13] Dang, F.; Tabata, O.; Kurokawa, M.; Ewis, A. A.; Zhang, L.; Yamaoka, Y.; Shinohara,

S.; Shinohara, Y.; Ishikawa, M.; Baba, Y. *Anal. Chem.* **2005**, *77*, 2140-2146.

[14] Tsao, C-W.; De Voe, D. L. *Microfluid Nanofluid.* **2009**, *6*, 1–16.

[15] Chung, Y. C.; Jan, M. S.; Lin, Y. C.; Lin, J. H.; Cheng, W. C.; Fan, C. Y. *Lab Chip* **2004**, *4*, 141–147.

[16] Bhattacharyya, A.; Klapperich, C. M. *Anal. Chem.* **2006**, *78*, 788–792.

[17] Karwa, M.; Mitra, S. *Polym. Prepr. (Am. Chem. Soc., Div. Polym. Chem.)* **2006**, *95*, 357.

[18] Sauer-Budge, A. F.; Mirer, P.; Chatterjee, A.; Klapperich, C. M.; Chargin, D.; Sharon, A. *Lab Chip* **2009**, *9*, 2803-2810.

[19] Witek, M. A.; Hupert, M. L.; Park, D.; Fears, K.; Murphy, M. C.; Soper, S. A. *Anal. Chem.* **2008**, *80*, 3483-3491.

[20] Xu, Y.; Vaidya, B.; Patel, A. B.; Ford, S. M.; McCarley, R. L.; Soper, S. A. *Anal. Chem.* **2003**, *75*, 2975-2984.

[21] Cao, W.; Easley, C. J.; Ferrance, J. P.; Landers, J. P. *Anal. Chem.* **2006**, *78*, 7222-7228.

[22] Nakagawa, T.; Tanaka, T.; Niwa, D.; Osaka, T.; Takeyama, H.; Matsunaga, T. *J. Biotechnol.* **2005**, *116*, 105–111.

[23] Kim, J.; Gale, B. K. *Lab Chip* **2008**, *8*, 1516–1523.

[24] Hwang, K. Y.; Lim, H. K.; Jung, S. Y.; Namkoong, K.; Kim, J. H.; Huh, N.; Ko, C.; Park, J. C. *Anal. Chem.* **2008**, *80*, 7786-7791.

[25] Hwang, K. Y.; Jeong, S. Y.; Kim, Y. R.; Namkoong, K.; Lim, H. K.; Chung, W. S.;

Kim, J. H.; Huh, N. *Sens. Actuators, B* **2011**, *154*, 46–51.

[26] Absolom, D. R.; Lamberti, F. V.; Policova, Z.; Zingg, W.; van OSS, C. J.; Wilhelm Neumann, A. *Appl. Environ. Microbiol.* **1983**, *46*, 90–97.

[27] Cho, Y. K. ; Kim, J. T. ; Lee, Y. S. ; Kim, Y. A. ; Namkoong, K. ; Lim, H. K. ; Oh, K. W. ; Kim, S. H. ; Han, J. I. ; Park, C. S. ; Pak, Y. E. ; Ki, C. S. ; Choi, J. R. ; Myeong, H. K. ; Ko, C. *Biosens. Bioelectron.* **2006**, *21*, 2161-2169.

[28] Abgrall, P.; Gue, A-M. *J. Micromech. Microeng.* **2007**, *17*, R15–R49.

[29] Eddings, M.A.; Johnson, M.A.; Gale, B. K. *J. Micromech. Microeng.* **2008**, *18*, 067001 1-4.

[30] Bhattacharya, S.; Datta, A.; Berg, J. M.; Gangopadhyay, S. *J. Microelectromech. Syst.* **2005**, *14*, 590-597.

[31] Truckenmuller, R.; Ahrens, R.; Cheng, Y.; Fischer, G.; Saile, V. *Sens. Actuators, A* **2006**, *132*, 385–392.

[32] Truckenmuller, R.; Henzi, P.; Herrmann, D.; Saile, V.; Schomburg, W. K. *Microsyst. Technol.* **2004**, 10, 372–374.

[33] Carp, O.; Huisman, C. L.; Reller, A. *Prog. Solid State Chem.* **2004**, *32*, 33-177.

[34] Kubo, W.; Tatsuma, T.; Fujishima, A.; Kobayashi, H. *J. Phys. Chem. B* **2004**, *108*, 3005-3009.

[35] Yu, H. W.; Lee, C. H.; Jung, P. G.; Shin, B. S.; Kim, J. H.; Hwang, K. Y.; Ko, J. S. *J. Micro/Nanolith. MEMS MOEMS.* **2009**, *8*, 021113 1-7.

[36] Rasmussen, R.; Morrison, T.; Herrmann, M.; Wittwer, C. *Biochemica* **1998**, *2*, 8-11.

Chapter 4. Miniaturized bead-beating device to automate full DNA sample preparation processes for gram-positive bacteria

4-1. Introduction

Nucleic acid-based micro total analysis system (μTAS) is a promising molecular diagnosis approach since entire analytical procedures (*i.e.*, sample preparation, amplification, and detection) are integrated and automated on a microchip format [1-3]. Real-time polymerase chain reaction (RT-PCR) has been widely accepted as both amplification and detection techniques because it provides higher accuracy and wider dynamic range than conventional PCR by determining the threshold cycle (Ct) directly proportional to the initial copy number. Moreover, it facilitates the integration of PCR technique into a microfluidic system by removing post-PCR processes such as sample transfer, reagent addition, gel-electrophoresis and fluorescence imaging [1, 4, 5]. However, DNA sample preparation process to acquire PCR-quality DNA from the raw samples remains as a critical hurdle toward the integration of full analytical steps into μTAS [6-8]. In order to achieve the successful amplification, nucleic acids should be properly extracted from clinical samples without potential PCR inhibitors because they have a direct effect on PCR performance (*i.e.*, sensitivity and specificity) [9-11]. In

addition, it is highly desirable to have the capability of enriching target analyte from a large volume of initial sample (*e.g.*, mL) into a microchamber during the sample preparation processes. By doing so, the large sample volume will be properly interfaced with micro-scaled devices, which can increase the detection sensitivity through target analyte concentration. This would be one of the most important characteristics of μTAS which can compete with the conventional benchtop analytical methods. Therefore, incorporation of the above functions into the nucleic acid sample preparation device would be the key to the practical application of μTAS.

Among nucleic acids sample preparation steps, cell lysis is the fundamental step to release them by disrupting cell membrane. In particular, the gram-positive bacteria possess a thicker peptidoglycan layer in cell wall, and thus it is harder to lyze them than the gram-negative ones [12]. *Staphylococcus aureus* (*S. aureus*), *streptococcus pneumonia*, and *enterococcus* species, *etc.* are classified as gram-positive cells. They cause hospital-acquired infectious diseases such as MRSA (Methicillin-resistant *staphylococcus aureus*), VRE (Vancomycin-resistant *enterococcus*), and sepsis, *etc*. Although the mechanical or enzymatic methods have been largely employed to disrupt gram-positive bacteria [13-18]. their incorporation into the miniaturized platform remains challenging. For example, for the enzymatic lysis of *S. aureus* using a commercial Qiagen kit protocol [13], it requires at least two types of enzymes (lysostaphin and lysozyme), temperature control for enzyme reaction, and long processing time (*ca.* 2 hr). Further purification steps are needed because the left enzymes and some chemicals (EDTA and

detergents, *etc.*) are inhibitory to PCR amplification. These complex processes could not be easily installed in a microfluidic system.

In comparison, the mechanical lysis techniques such as bead-beating and ultrasonic methods are simpler and more efficient than the enzyme-based technique, despite that they require specialized laboratory instruments. Indeed, there have been some trials to implement the mechanical lysis into a microchip platform. For example, an ultrasonic horn was installed in an analytical system, which delivered an ultrasonic energy to disrupt bacterial cells [19-20]. Also, mechanical shearing effect was applied by flowing a liquid sample through porous polymer monolith or sharp microstructures under mixed chaotrope and detergent solution [21-22]. Nonetheless, a real active device based on "bead-beating" is still needed because the impact force occurring on bead collision along with shear effect is important to lyze gram-positive bacteria or yeast. This would be one of reasons why studies on detection sensitivity of gram-positive bacteria have been rarely reported with a microfluidic platform [21]. Although some attempts have been made on a centrifugal CD-based microfluidic device, their analytical performance such as detection sensitivity remains unknown [23-24]. In the context of microchip-based approach, a stand-alone flexible bead-beating chamber installed with an external actuator has been demonstrated to induce bead-beating cell lysis [25]

In this study, we have developed a bead-beating microdevice through the pneumatic vibration of elastomeric membrane (PDMS). It was fabricated by sandwiching a PDMS membrane between two glass chips (glass-PDMS-glass). In order to automate the full

DNA extraction processes efficiently, the proposed microdevice and biological protocol were designed to have the following features: First, a monolithic flexible PDMS membrane, typically used as a flow-regulating tool [26-27], was further employed as an actuator for bead collision *via* its pneumatic vibration. Namely, both manipulation of solutions (pumping and valving) and bead-beating for mechanical cell lysis were simultaneously implemented on a microchip using a single pneumatic source without any specialized lysis equipments. Also, valve seat and weir for bead trapping were designed to have the same microstructure, thereby simplifying the overall fabrication processes. In the aspect of biological protocol, surface-modified glass beads were used to capture bacterial cells, which also acted as a grinding media to disrupt the captured cells on their surface. Furthermore, the present microdevice transformed the captured cells from 1 mL of initial sample into an analyte volume of 10 or 20 μL DNA solution. It reduced the initial sample volume by 100 or 50-fold, thereby concentrating the target analyte into a microscale volume that is more compatible for subsequent PCR amplification. As a result, our microdevice showed an excellent DNA extraction performance similar to the conventional benchtop vortexing machine or enzymatic method, allowing for successful PCR detection of gram-positive bacteria. Here, we present analytical performance of the bead-beating device together with microfluidic integration for valving and pumping.

4-2. Experimental

4-2-1. Cell strain and culture

Bacterial strains used in this study were methicillin-susceptible *staphylococcus aureus* (ATCC No. BAA 1718, *S. aureus*) and methicillin-resistant *staphylococcus aureus* (ATCC No. 33591, MRSA). They were grown in 50 mL trypticase soy broth (Becton, Dickinson and Company) at 37 ℃ overnight and suspended to appropriate concentrations with sodium acetate buffer (pH 4, 50 mM) after washing twice with 1X PBS solution (pH 7.4). The optical density of 0.2 OD was found to be *ca.* ~10^8 CFU (colony forming unit)/mL.

4-2-2. Bead surface modification

Glass beads (Polysciences) with a diameter of 30 μm ~ 50 μm were cleaned in piranha solution. After thorough washing with DI water, they were filtered and vacuum-dried. The solution for bead surface modification was prepared to contain 5% (vol./vol.) of trimethoxysilylpropyl modified (polyethyleneimine) (Gelest) in ethanol. Glass beads were immersed in the prepared solution and allowed to react for 2 hrs with a gentle mixing. Afterwards, they were filtered and rinsed with the fresh ethanol. It was repeated three times. Finally, the recovered glass beads were incubated at 110 ℃ for 50 min.

4-2-3. Testing instrumentation

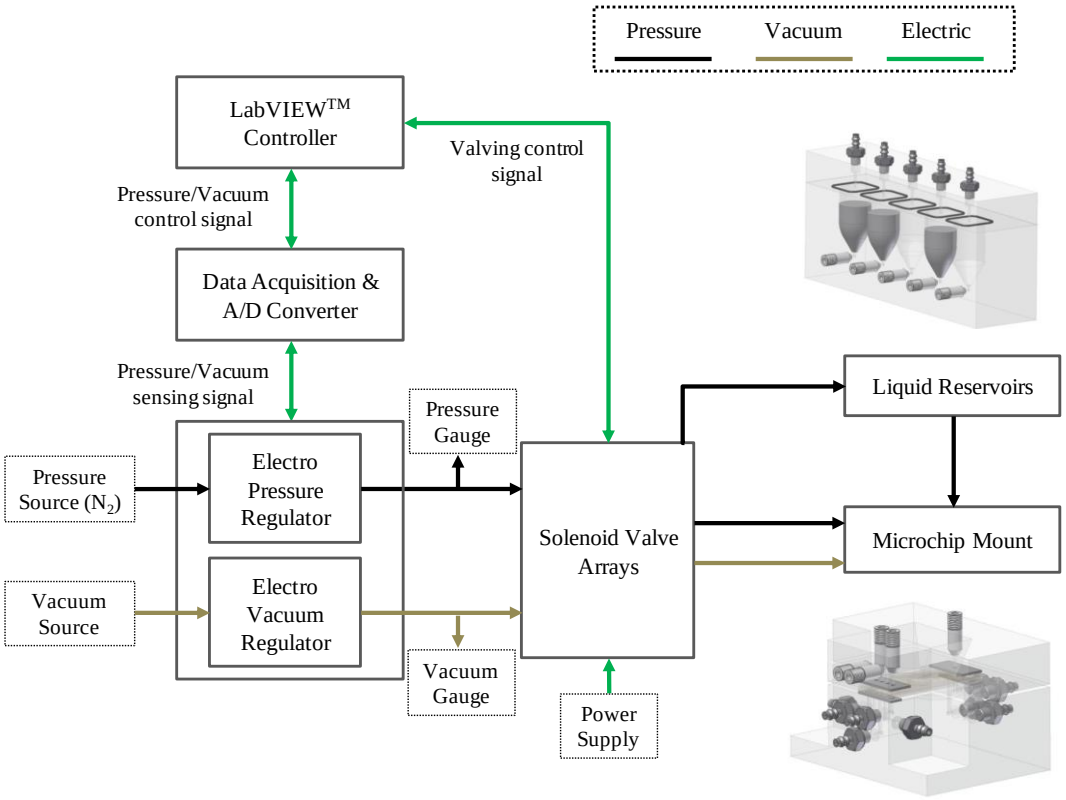

Figure 4-1. Experimental set-up for the automatic extraction of bacterial DNA

PDMS membrane operation was controlled by applying the positive or negative pressure in pneumatic displacement chambers through an array of solenoid valves (S070-5DC, SMC), which were interconnected with electro-pneumatic-regulator (ITV0030-3BL, SMC) and LabVIEW software (National Instruments). The valve operation coupled with fluid transport was visualized at each step in the LabVIEW interface to monitor nucleic extraction procedure. The testing instrument to automate DNA extraction processes was constructed as shown in Figure 4-1.

4-2-4. Device fabrication

Microfluidic features such as valve seats and channels were fabricated on a glass wafer using conventional photolithography and wet etching techniques [26-27]. Briefly, 6-inch borosilicate glass wafers (700 μm thickness) were piranha-cleaned and 500 nm of amorphous polysilicon was deposited using a low pressure chemical vapor deposition. Then, the wafers were coated with photoresist, patterned, and developed. The exposed polysilicon layer was dry-etched, the photoresist was stripped, and the resulting exposed glass was isotropically etched to have a final depth of *ca.* 100 μm and width of *ca*. 200 μm with HF (hydrofluoric acid, 49%) solution. After removing the remained polysilicon, the glass wafers were patterned with dry film resist on the etched side, and then the bead chamber and holes (fluidic and pneumatic access) were generated by sand-blasting technique. The bead chamber and its corresponding pneumatic displacement chamber

were an oval type. The bead chamber had the volume of *ca.* 15 μL and the size of *ca.* 6 mm × 4 mm × 0.75 mm (Longest × Shortest × Depth), respectively. The two pneumatic displacement chambers for bead-beating had the total volume of *ca.* 3 μL and the size of *ca.* 6 mm × 4 mm × 0.2 mm (Longest × Shortest × Depth), respectively, and the spacing between two wells was *ca.* 0.4 mm. The manufactured glass wafers were diced into chips (27.4 mm × 12 mm). The resulting fluidic and pneumatic manifold chips were plasma-cleaned (Harrick) and bonded permanently by sandwiching plasma-activated PDMS membrane sheet (254 μm thickness, Rogers). About 15~16 mg of surface-modified glass beads were weighed within the bead chamber and PCR-compatible adhesive tape (Applied biosystems) was sealed to close the open chamber. The polycarbonate plate (1 cm × 1 cm × 0.7 cm) was additionally glued over the adhered adhesive tape to prevent its deflection during DNA extraction processes.

4-2-5. DNA extraction

1 mL of sodium acetate buffer (50 mM, pH 4, Sigma-Aldrich) containing *S. aureus* or MRSA (typically 10^6 CFU/mL), 0.5 mL of TE buffer (10 mM, pH 8, Ambion) for washing, and 10 μL or 20 μL of NaOH solution (0.02 N, Sigma-Aldrich) for lysis were previously dispensed into liquid reservoirs. The liquid solutions were transported in a pressure-driven manner and their operating fluid pressures were determined in preliminary experiments. The initial sample solution passed through the bead-packed

chamber with a flow rate of *ca.* 200 μL/min at 30 kPa while pressurizing PDMS membrane of bead chamber upward at 150 kPa. The flown-through solution was recovered to evaluate the cell capture capability. After initial loading, the bead-packed chamber was washed at a flow rate of *ca.* 500 μL/min (80 kPa), and N_2-dried for 30 sec with 100 kPa. For lyzing the captured cells, 6 μL of NaOH was injected and valves at both sides of bead-packed chamber were closed. The pressures of two pneumatic displacement chambers alternate asynchronously with one chamber positive (80 kPa) and the other negative (-80 kPa) for the first half a cycle and they were reversed for the second half a cycle. PDMS membrane vibrated at a frequency of 10 Hz for 5 min. The extracted DNA was eluted by injecting another 4 μL or 14 μL of NaOH solution with a fluid pressure of 100 kPa, and 10 μL or 20 μL of DNA solution was obtained as a result. The overall process time took less than 20 min. No further DNA purification steps were performed. Detailed description of microdevice components was provided in the Figure 4-2.

4-2-6. Positive and negative lysis controls (benchtop DNA extraction)

Two types of benchtop lysis techniques (*i.e.*, enzymatic and bead-beating methods) were carried out as a positive lysis control (PLC). 1 mL of *S. aureus* samples having two different cell concentrations (10^4 CFU/mL and 10^6 CFU/mL) were centrifuged in microcentrifuge tubes at 13,200 rpm for 20 min and the supernatant was carefully

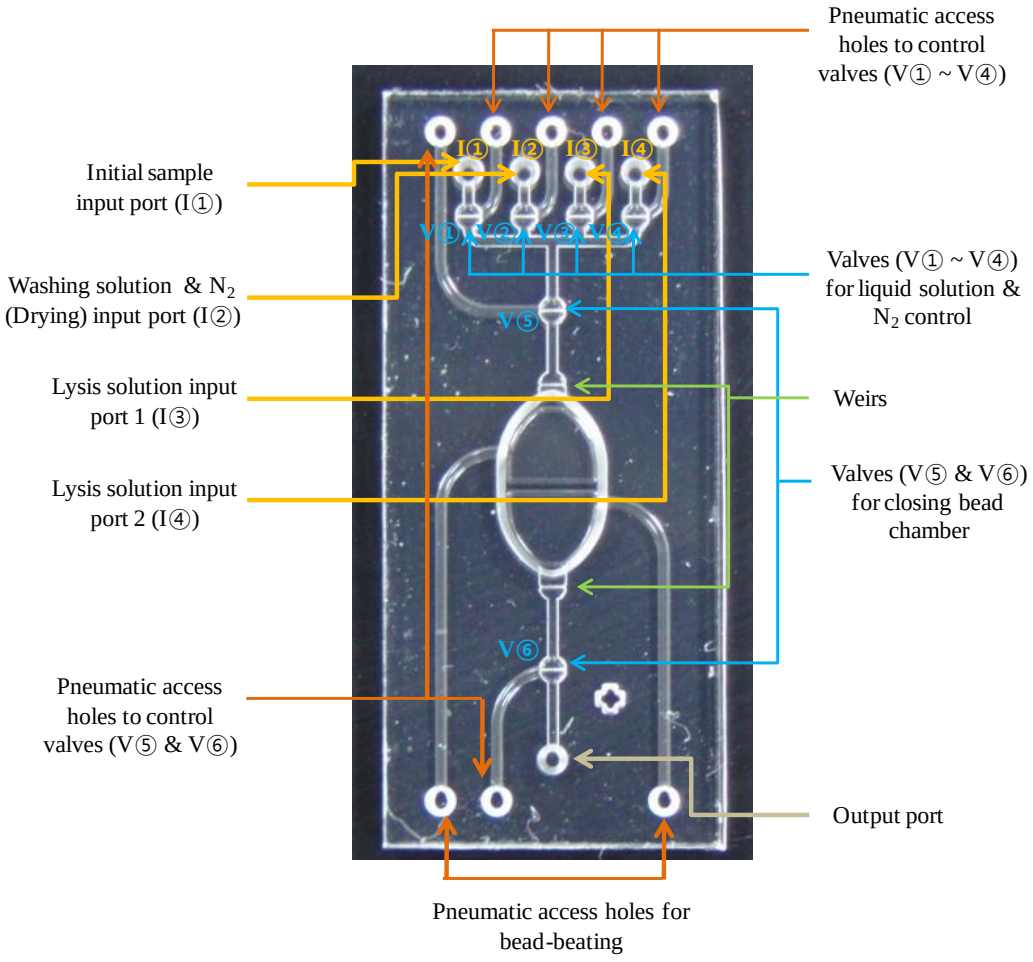

Figure 4-2. Detailed description of microfluidic components in bead-beating microdevice.

discarded. The remained cell pellets were further treated with the above techniques, respectively. In the case of an enzymatic method, the cell pellet was incubated with lysostaphin solution (200 μg/mL, Sigma) at 37 ℃ for 30 min before application to the Qiagen DNA extraction kit (Cat 51304, QIAamp DNA Mini Kit), and 20 μL of purified DNA solution was acquired as described in its protocol. For a benchtop bead-beating lysis, after adding both 30 mg of bare glass bead and 20 μL of lysis solution (0.02 N NaOH solution or DI water) to cell pellet, vortexing was vigorously performed at the full speed for 5 min (GENIE 2, Fisher Scientific). The extracted DNA solution was recovered following brief centrifugation. As a negative lysis control (NLC), the cell pellet was vortexed with DI water only (in the absence of glass beads). The resulting lysis control samples (PLC and NLC) were amplified in comparison with the obtained DNA solution from the bead-beating microdevice. For the accurate comparison, the total number of *S. aureus* injected and final DNA elution volume were always controlled to be the same with those samples.

4-2-7. Real-time PCR amplification

In order to evaluate the cell lysis performance and the resulting extracted DNA quality, real-time PCR (polymerase chain reaction) assays were performed on the GenSpector® TMC-1000 instrument (Samsung Electronics) [5]. Primer sets specific to SA442 region (forward: 5'- GTT GCA TCG GAA ACA TTG TGT - 3' and reverse: 5'-

ATG ACC AGC TTC GGT ACT ACT AAA GAT - 3', GeneBank accession number AF033191) of *S. aureus* genome and mecA fragment (forward: 5'- ACG AGT AGA TGC TCA ATA - 3' and reverse: 5'- GGA ATA ATG ACG CTA TGA T - 3', GeneBank accession number EF190335.1) of MRSA genome were designed by Primer3 software (Whitehead Institute/MT Center for Genome Research), respectively. PCR reaction mixture (*ca.* 2 μL) was prepared to possess the following final concentrations: 0.4 μM Taqman probe (FAM - 5' - TGT ATG TAA AAG CCG TCT TG - 3' - MGB - NFQ for *S. aureus* and FAM - 5' - CCA ATC TAA CTT CCA CAT ACC ATC T - 3' - BHQ1 for MRSA, respectively), 1X Z-Tag buffer (Takara Bio), 1 μM each primer (Applied Biosystems or Sigma), 0.05 U Z-Taq polymerase (Takara Bio), 0.2 mM dNTP (Takara Bio), 0.5 μL PCR grade water (Ambion), and 1 μL extracted DNA solution. After loading into PCR chip, the thermocycling was performed with a denaturation step at 95 ℃ for 1 sec and an extension step at 60 ℃ for 4 sec. The size of PCR amplicons were designed to be 72 and 98 base pairs for *S. aureus* and MRSA, respectively. They were further confirmed by gel-electrophoresis (Agilent 2100 Bioanalyzer, Agilent Technologies).

4-3. Results and Discussion

4-3-1. Device layout and characterization

The bead-beating microdevice presented here is based on monolithic integration of

polymer membrane valve and two glass layers [25-26]. It consists of fluidic (top glass), PDMS, and pneumatic (bottom glass) layers, which is schematically illustrated in Figure 4-1. About 15 μL of cell lysis chamber was constructed to accommodate surface-modified glass beads in the fluidic layer so that they were in direct contact with liquid solutions. The installed glass beads were designed to act both as cell capture and grinding media. In order to establish the bead-beating operation within a microfluidic platform, pneumatic vibration of PDMS membrane was carried out to actuate glass beads, thereby inducing vigorous collision and shear stress. Two pneumatic displacement chambers were fabricated to apply a positive and a negative pressure alternatively. In addition, the PDMS membrane was permanently bonded to the two glass wafers because the previous reversible bonding has shown limitations on valve operation under a fluid pressure of 75 kP [26-27]. Because the plasma-activated irreversible PDMS bonding causes typical PDMS sticking onto valve seat, the valve seat was isotropically etched to be separated from the PDMS mating surface by *ca.* 20 μm (See Figure 4-3a, 4-4 & 4-5). It turned out that the suggested alteration on membrane valve structure made it operable in a wider range of fluid pressures (~ 300 kPa) without any solution leakage and membrane sticking [28]. Moreover, the same isotropically-etched microstructures were also used as weirs to isolate the glass beads (*ca.* 30 μm ~ 50 μm) within the microchamber (Figure 4-3a & 4-4c). Such dual-functional device components could make possible facile construction of operating components as well as simplification of fabrication processes.

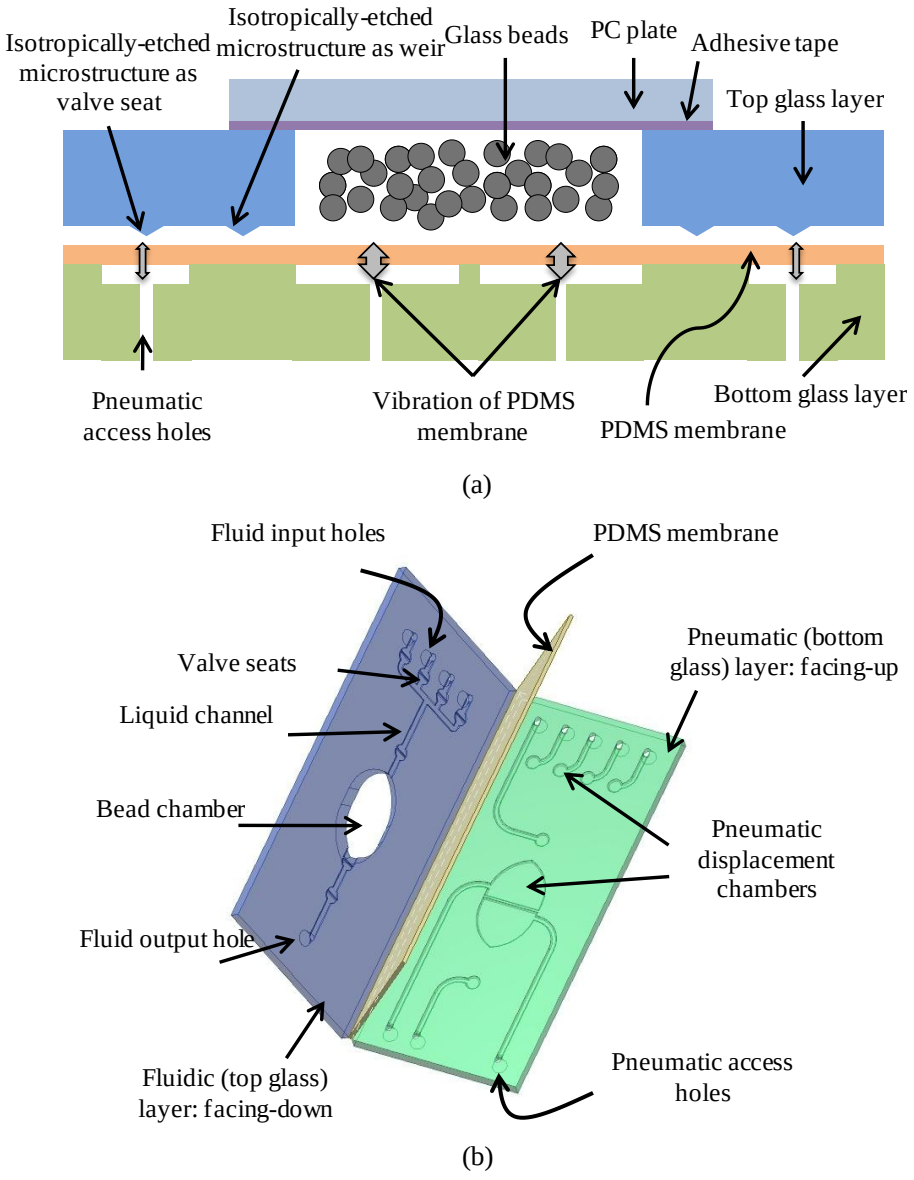

Figure 4-3. (a) Cross-sectional view of the miniaturized bead-beating device *via* vibration of PDMS membrane. (b) Exploded view of the three-layer monolithic glass-PDMS-glass microdevice and its fluidic and pneumatic components.

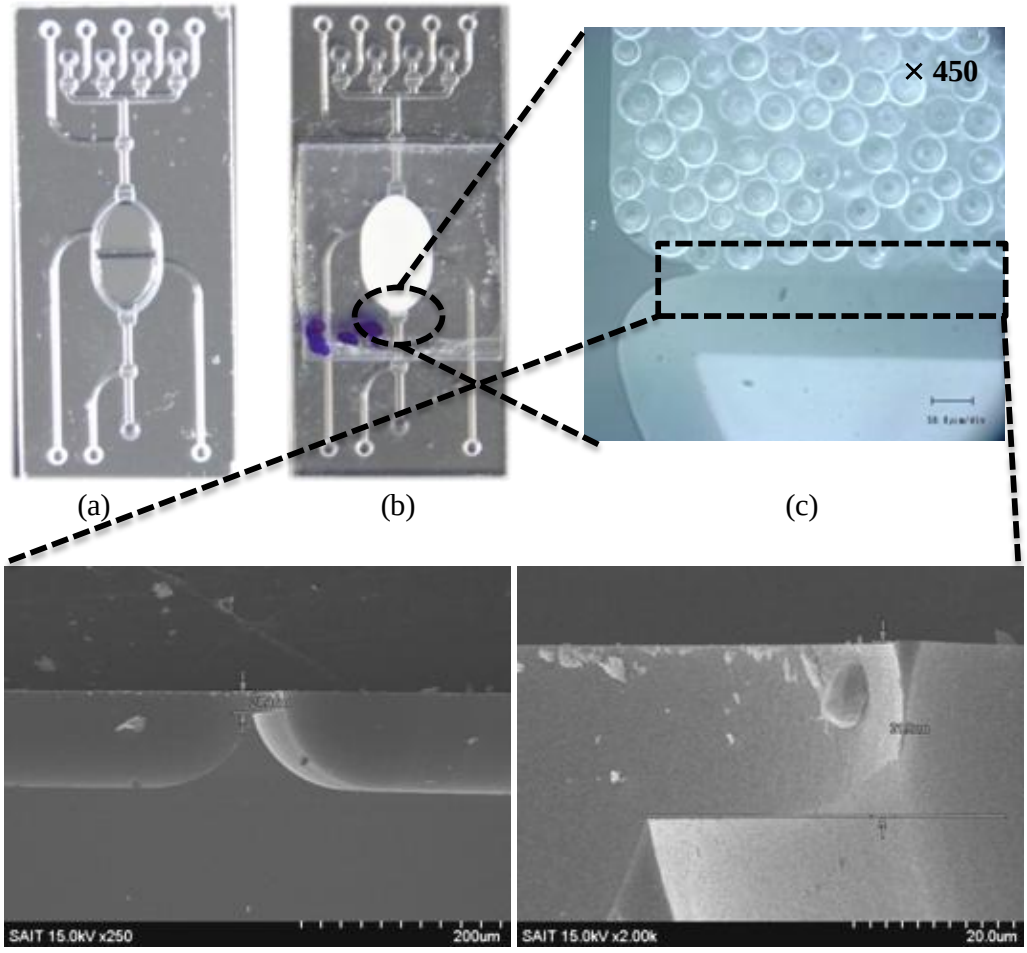

Figure 4-4. Digital pictures and SEM images of the fabricated bead-beating microdevice: (a) assembled microchip through PDMS-interface bonding (27.4 mm × 12 mm), (b) sealed microchip packed with glass beads (*ca.* 30 ~ 50 μm), (c) one of isotropically-etched microstructure working as a weir for isolating glass beads, and (d) etching depth of *ca.* 20 μm from the bonding surface.

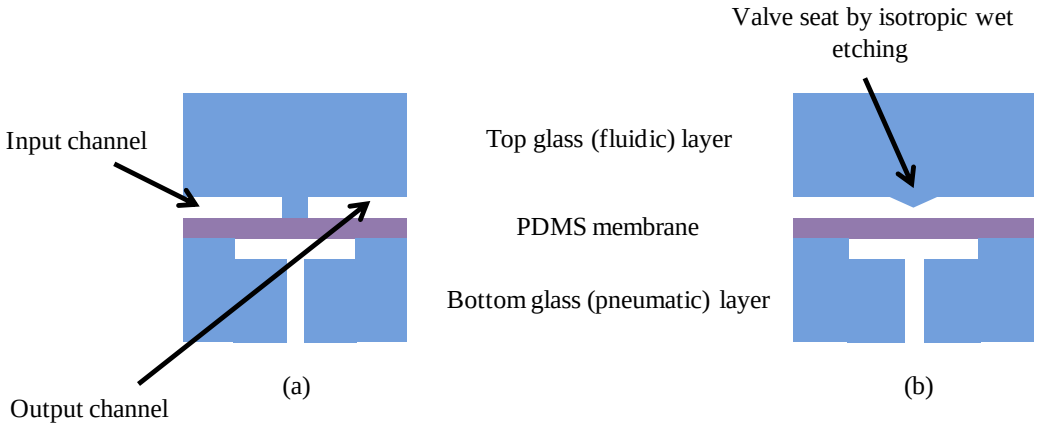

Figure 4-5. Cross-sectional illustration view of the membrane valve structure: (a) PDMS sticking onto valve seat (normally-closed type) with plasma-activated permanent bonding, and (b) isotropically-etched valve seat (normally-half-open type) to prevent PDMS sticking.

4-3-2. Evaluation of PLC samples (benchtop DNA extraction)

The threshold cycle (Ct) values of PLC samples were obtained as shown in Table 4-1. Generally, the benchtop bead-beating method has been applied in combination with lysis solution containing detergent or chemical to enhance lysis efficiency. Here, NaOH solution (0.02 N) was chosen because it did not inhibit PCR amplification at all without further purification steps (data not shown). The effect of bead-beating was more distinct with NaOH solution than DI water, suggesting that NaOH contributed to DNA extraction yield by disrupting cell membrane chemically. For enzymatic lysis of *S. aureus*, lysostaphin was utilized because it is capable of specifically cleaving the crosslinking pentaglycine bridges in the cell walls of *staphylococci* [13, 29]. As shown in the Table 4-1, the benchtop bead-beating method with NaOH solution performed better than or similar to the enzyme-based DNA extraction in terms of Ct values. Therefore, the performance of miniaturized bead-beating device was evaluated by comparing it to the benchtop vortexing machine. As the measurement of optical density is a rough cell quantification technique, the Ct value of PLC was varied daily with a standard deviation of *ca.* 1.5 even at the identical optical density. For comparison, the NLC vortexed with DI water only showed Ct of *ca.* 31.5 and *ca.* 37.0 for 10^6 CFU/mL and 10^4 CFU/mL samples, respectively.

4-3-3. Cell capture

Table 4-1. Ct values of PLC samples.

Number of applied *S. aureus* cell (CFU)	Benchtop bead-beating method		Enzymatic method (Lysostaphin)
	NaOH (0.02 N)	DI water	
~ 10^4	30.5 ± 0.35	34.5 ± 0.26	31.6 ± 0.56
~ 10^6	23.7 ± 0.29	26.7 ± 0.15	25.7 ± 1.43

Three repetitions were performed for each cell number.

The basic operation of the present microdevice is as follows: (1) cell capture on glass beads, (2) washing & drying, (3) cell lysis using *in-situ* bead-beating, and (4) elution of extracted DNA solution. The bacterial cells can be captured on the solid substrate in specific or non-specific manners. Along with the cell-specific immunoaffinity technique [30-31], nonspecific cell capture methods using surface thermodynamics [32-34] or electrostatic interaction [35-37] have demonstrated their ability to capture pathogenic bacteria. In this work, the long-range Coulombic electrostatic interaction [35-37] was exploited by modifying glass beads electropositive. Specifically, the surface of glass beads was derivatized so as to possess the positive amine groups in reaction with organosilane compound containing polyethyleneimine. After packing the surface-modified glass beads inside of the microchamber (Figure 4-4), 1 mL of initial sample solution with *S. aureus* (10^6 CFU/mL) passed through them. At first, the role of electrostatic interaction was assessed by comparing the modified glass beads with the bare ones. It was found that the Ct value of eluted DNA from the modified glass beads was lower than that of unmodified ones by 2. These results indicated that the cell capture efficiency was greatly increased with the surface modification by a factor of 4 (*i.e.*, 1 Ct difference indicates 2-fold difference in initial template copy numbers). To obtain a more quantitative comparison on cell capture capability, the passed-through sample solution was collected at the outlet of microdevice. Then, *S. aureus* in the solution, not captured on the bead surface, was subject to benchtop vortexing with bare glass beads as with the case of PLC samples. The Ct value of passed-through *S. aureus* was compared to that of

the eluted DNA solution obtained from the operation of bead-beating microdevice. Finally, their Ct difference was used as a measure to estimate the cell capture efficiency and capacity. When 1 mL of the various concentrations of *S. aureus* (10^4, 10^5, 10^6, 10^7, and 10^8 CFU/mL) was applied, Ct difference was maintained to be over 5 in the range of 10^3 CFU/mL to 10^7 CFU/mL and it dropped to about 2.5 for the 10^8 CFU/mL. Therefore, the capture efficiency would be over 90% as evidenced by the ten-fold difference in the initial template copy numbers accompanying the Ct change of *ca.* 3.3 (*i.e.*, verified while evaluating the limit of detection in the final section). In addition, the cell capture efficiency was further confirmed by the colony count method [32, 34]. It appears that the fabricated bead-packed microdevice displays the capacity over ~ 10^7 CFU of *S. aureus*. After cell capture, the bead-packed microchamber was washed and N_2-dried such that the complete exchange to lysis solution was achieved. These results demonstrated the potential of *in-situ* bead-beating lysis of the captured cells instead of releasing them. Other cell capture techniques such as immunoaffinity-based ones can also be incorporated in the present device by adopting proper solid surface modification chemistry.

4-3-3. Miniaturized bead-beating lysis

The bead-beating cell lysis takes place when the captured cells on bead surface are disrupted by inter-bead collision or shear effect. Some controllable parameters are conceivable that can affect bead motion such as membrane vibration frequency (5 Hz ~

10 Hz), membrane actuation pressure (20 kPa ~ 80 kPa), and depth of pneumatic displacement chamber (100 μm ~ 200 μm). When the bead chamber is fully filled with the lysis solution, it turned out that the above parameters did not improve the cell lysis efficiency notably on the basis of the PCR Ct values (data not shown). From these results, it could be thought that the incompressible liquid solution would inhibit the membrane deflection and bead motion in a confined chamber, which fails to induce the bead-beating lysis. To investigate the effect of liquid amount participating in the bead-beating lysis, the liquid volume fraction (f_L) was defined as the ratio of lysis solution volume to void volume of lysis chamber. The void volume of lysis chamber was calculated to be *ca.* 12 μL by subtracting net volume of glass bead (*ca.* 6 μL) from that of lysis chamber (*ca.* 18 μL, including pneumatic displacement volume of the chamber). The final eluted DNA volume was controlled to be the same (20 μL) by adjusting the additional NaOH solution when eluting the extracted DNA from the bead chamber. As shown in Figure 4-6, f_L was found to be the key factor to determine PCR Ct values. The Ct value became close to that of PLC when f_L approached *ca.* 0.3.

To gain an understanding on this behavior, an attempt was made to separate the bead-beating and chemical effect from the obtained lysis results. Use of DI water instead of NaOH appears the most direct way to exclude the effect of chemical lysis caused by NaOH. However, it was hindered by the fact that the extracted DNA (*i.e.*, containing phosphate groups) adsorbed significantly on the positively-charged bead surface at neutral pH (*i.e.*, Ct was *ca.* 28). These results implied that NaOH neutralized the bead

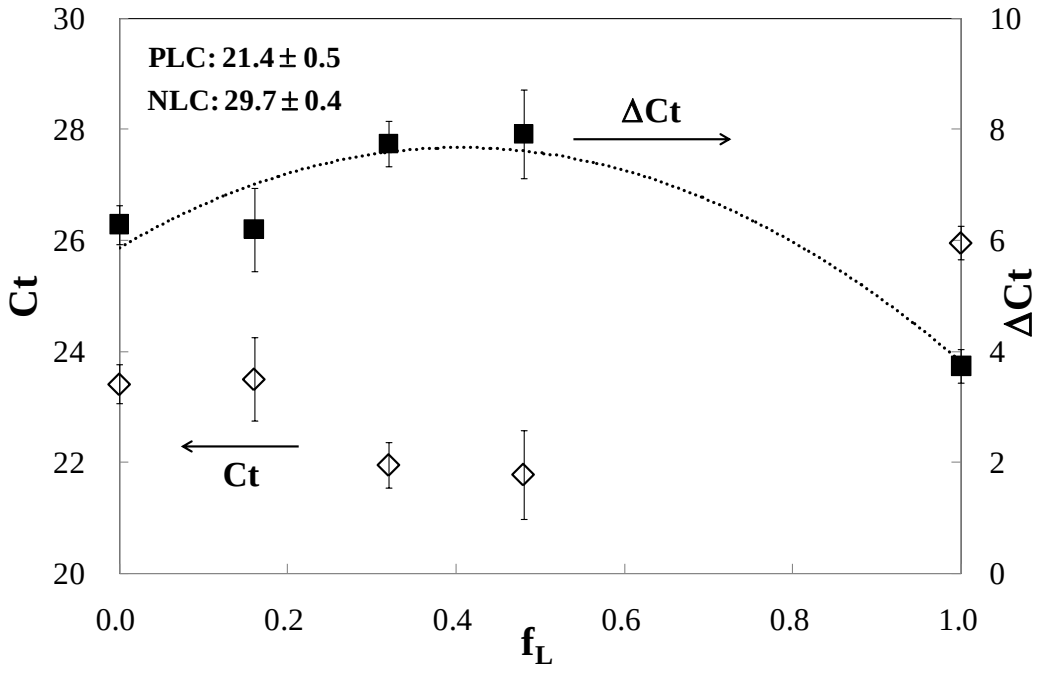

Figure 4-6. Effect of liquid volume fraction (f_L) on bead-beating lysis in the fabricated microdevice. (a) Obtained Ct values (◇) and ΔCt (NLC Ct – Ct, ■) as a function of f_L. Three repetitions were performed for each f_L. 1 mL of *S. aureus* (10^6 CFU/mL) was applied.

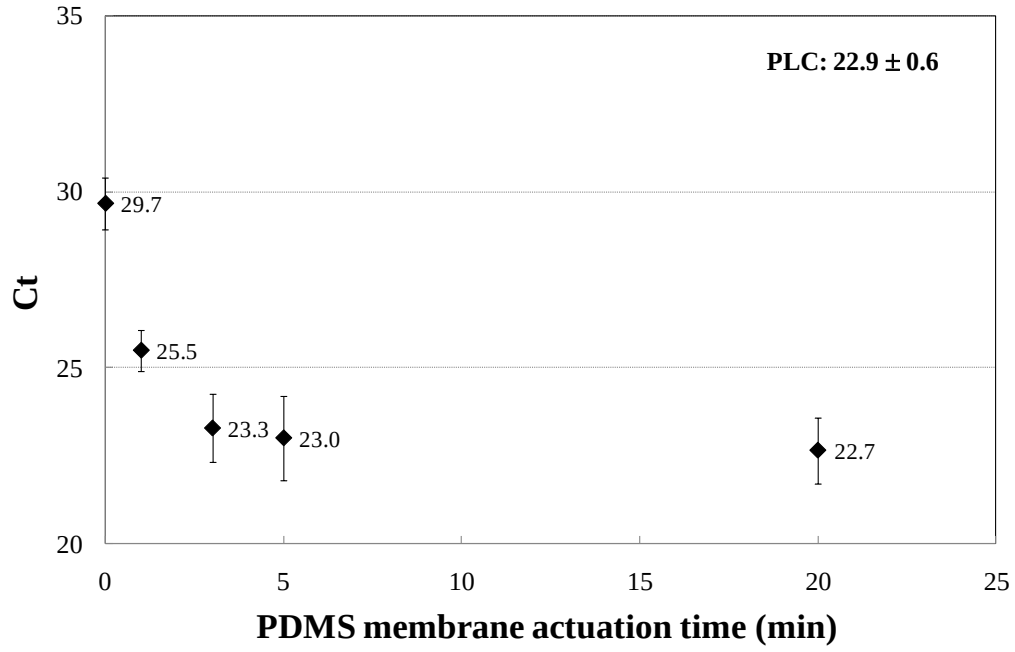

Figure 4-7. Ct values as a function of PDMS membrane actuation time. 1 mL of *S. aureus* (10^6 CFU/mL) was applied. Three repetitions were performed for each actuation time.

surface by increasing the solution pH above pKa of amine groups and induced the cell membrane breakage to some extent. Thus, NaOH-driven chemical lysis was indirectly estimated from the cell pellet as with the case of PLC. Lysis with NaOH without beads yielded *ca.* 3 Ct decrease (*i.e.*, the maximum chemical lysis effect) from NLC Ct, which turned out to be almost equivalent to ΔCt decrease (*ca.* 3.7, NLC Ct – Ct) when f_L = 1 (Figure 4-6). These results indicated that the bead-beating lysis was nearly negligible when the lysis chamber was full of NaOH solution. Also, Ct at f_L = 0 would represent the bead-beating lysis only without chemical effect. The effect of chemical lysis would increase with increasing f_L until NaOH solution soaks the entire surface of glass bead. Assuming that packing ratio of glass beads is 50% when PDMS membrane presses them upward, 6 μL of lysis solution is required to soak the whole glass bead surface, which corresponds to f_L of *ca.* 0.5 (*i.e.*, 6 divided by 12). Also, this would be the maximum f_L value where the membrane deflection was not hindered by the liquid solution because there was void space to accommodate it. However, Ct value approaching that of PLC at *ca.* f_L = 0.3 indicates that NaOH-driven chemical lysis would start to be saturated at this point. As f_L was increased from *ca.* 0.5 to 1, the increasing incompressible liquid solution would start to disturb the vibration of membrane. Therefore, the maximum cell lysis efficiency would be achieved with f_L in the range of 0.3 and 0.5 by maximizing both bead-beating cell lysis caused by membrane deflection and NaOH-driven chemical lysis. On the basis of these results, all subsequent experiments were performed by adjusting f_L at *ca.* 0.5.

4-3-4. DNA extraction using miniaturized bead-beating lysis

We further characterized the bead-beating microdevice by investigating the effect of PDMS actuation time and limit of detection (LOD). At first, the real-time PCR results were displayed as a function of PDMS actuation time (See Figure 4-7). It was observed that most of captured cells on beads surface was lyzed within 3 min (*i.e.*, its Ct value became close to PLC samples) and further actuation did not influence Ct significantly. Considering both cell capture and lysis performance, it could be inferred that a considerable degree of the achieved 50-fold volume reduction was translated into DNA enrichment effect. In order to measure the LOD, 1 mL of serially-diluted *S. aureus* samples (10^5, 10^4, 10^3, 10^2 CFU/mL and 0 CFU/mL) were applied and 20 μL of DNA solution was obtained. Until now, the attempt to detect gram-positive bacteria on a miniaturized platform has been rarely made, and even its reported detection sensitivity was lower than that of gram-negative bacteria by one or two orders-of-magnitude [21]. As shown in Figure 4-8a, the typical S-curved shape of PCR amplification was obtained for the tested samples, and furthermore 10^2 CFU samples were successfully detected. 0 CFU/mL and no template control (PCR-grade water) samples were not amplified. These results suggest that the *in-situ* bead-beating lysis in combination with flow-through cell capture could increase the effective analyte concentration, allowing for higher detection sensitivity for the gram-positive bacteria. Such target analyte enrichment is one of the potential benefits of the beat-beating microdevice, which was fully exploited in the

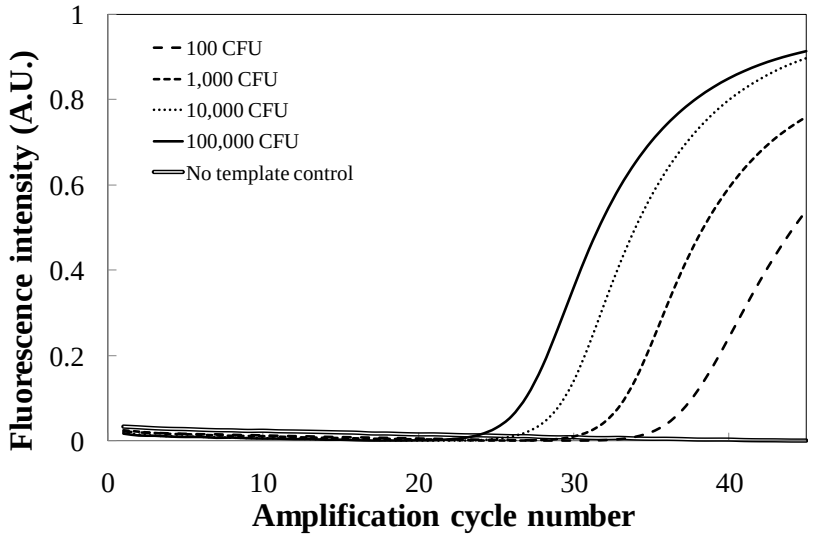

(a)

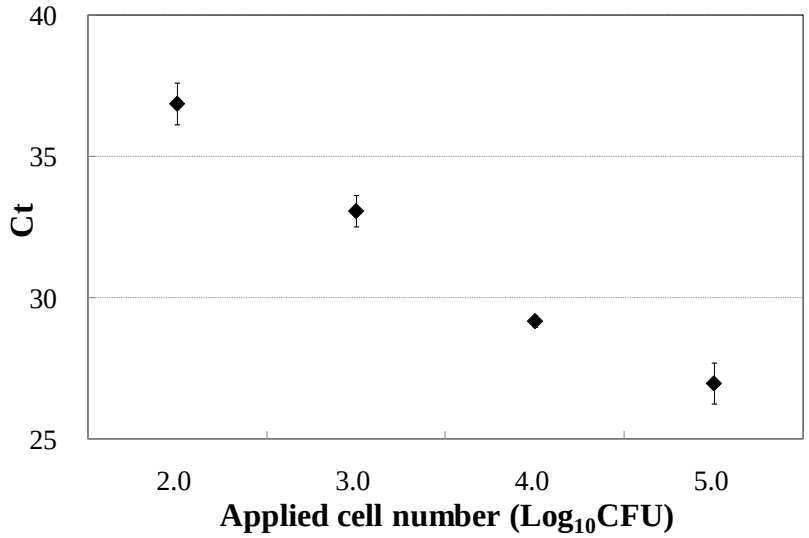

(b)

Figure 4-8. Real-time PCR detection of *S. aureus* using the bead-beating microdevice: (a) representative real-time PCR amplification curves and (b) obtained Ct values as a function of the applied *S. aureus* number. Three repetitions were performed for each cell number.

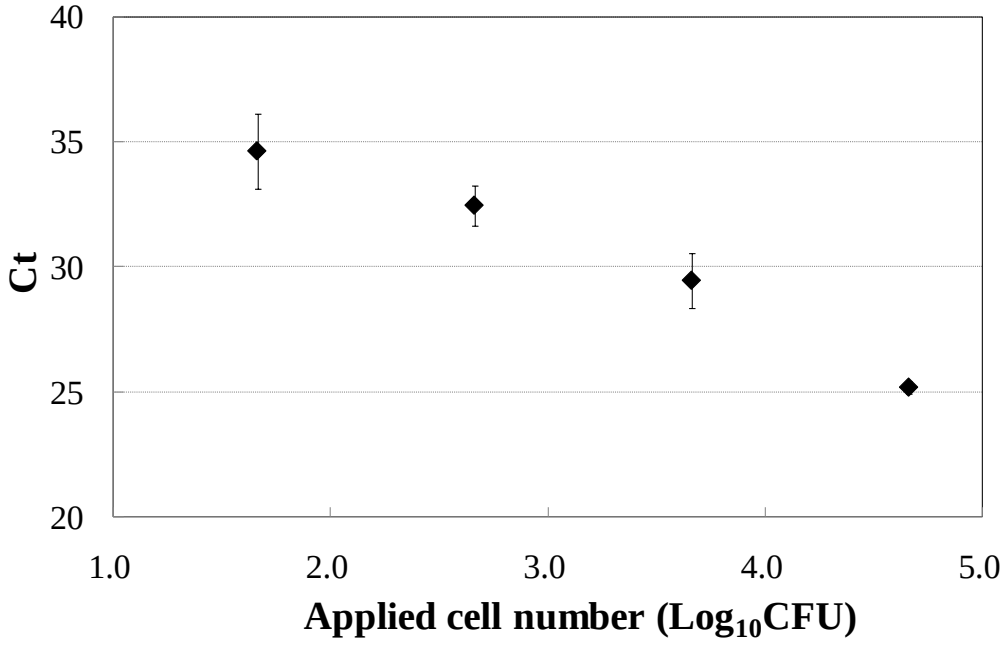

Figure 4-9. Real-time PCR detection of MRSA using the bead-beating microdevice in a high background of *S. aureus*. Three repetitions were performed for each cell number.

present approach. Noting that the cycle interval separating each 10-fold difference in initial template concentration was calculated to be about 3.36 (Figure 4-8b), a PCR efficiency, defined as the (number of copies at cycle n+1) / (number of copies at cycle n), was as high as 1.9 [38].

Lastly, we validated the present microdevice by detecting the low number of MRSA in a high background of *S. aureus*, which is closer to the complex clinical samples. Various amounts of MRSA were mixed with the constant amount of *S. aureus* (10^5 CFU/mL) to have the final MRSA concentrations of 4.6×10^4, 4.6×10^3, 4.6×10^2, 4.6×10^1 and 0 CFU/mL. For this test, 1 mL of initial sample was introduced and DNA was extracted with a total volume of 10 μL, and therefore 100-fold volume reduction was achieved. The total bacterial DNA (*S. aureus* and MRSA) was recovered and mecA region of MRSA was amplified. As shown in Figure 4-9, the detection of extremely low number of MRSA, *ca.* 46 CFU, was successfully demonstrated. The sample possessing 0 CFU of MRSA was not amplified. Also, these results implied that the non-specific cell capture would be applicable to PCR-based diagnostic system because the specificity could be derived from PCR. The installation of the bead-beating cell lysis technique into flow-through microdevice is capable of processing large sample volume allowed for the excellent detection performance for gram-positive bacteria. Application to the detection of MRSA in nasal swab is in progress.

4-4. Summary

In this chapter, we have demonstrated a miniaturized bead-beating device to lyze gram-positive bacteria by means of the vibration of monolithic PDMS membrane. The PDMS membrane was designed to be dual-functional as a valving component as well as a bead actuator, so that the single pneumatic source coupled with solenoid valves could implement the fluidic manipulation of liquid samples and bead-beating lysis without any additional specialized lysis equipment. The flow-through cell capture on glass beads from large sample volume and subsequent *in-situ* bead-beating lysis of captured cells on its surface gave rise to the significant DNA enrichment, which was translated into the high detection sensitivity (*ca.* 46 CFU) even for the gram-positive bacteria. Also, the liquid volume fraction played a crucial role in producing the maximum DNA yield because it dominated the membrane deflection, bead motion, and ultimately lysis capability. The bead-beating microfluidic device presented here is potentially useful for the development of μTAS aiming at the detection of various pathogens including gram-positive bacteria.

References

[1] Chen, L.; Manz, A. ; Day, P. J. R. *Lab Chip* **2007**, *7*, 1413-1423.

[2] Chin, C. D. ; Linder, V. ; Sia, S. K. *Lab Chip* **2007**, *7*, 41-57.

[3] Manz, A.; Graber, N.; Widmer, HM. *Sens. Actuators, B* 1990, **1**, 244-248.

[4] Higuchi, R.; Fockler, C.; Dollinger, G.; Watson, R. *Bio/Technology* **1993**, *11*, 1026–1030.

[5] Cho, Y. K. ; Kim, J. T. ; Lee, Y. S. ; Kim, Y. A. ; Namkoong, K. ; Lim, H. K. ; Oh, K. W. ; Kim, S. H. ; Han, J. I. ; Park, C. S. ; Pak, Y. E. ; Ki, C. S. ; Choi, J. R. ; Myeong, H. K. ; Ko, C. *Biosens. Bioelectron.* **2006**, *21*, 2161-2169.

[6] Huang, Y.; Mather, E. L.; Bell, J. L.; Madou, M. *Anal. Bioanal. Chem.* **2002**, *372*, 49–65.

[7] Lichtenberg, J.; De Rooij, N. F.; Verpoorte, E. *Talanta* **2002**, *56*, 233–266.

[8] Price, C. W.; Leslie, D. C.; Landers, J. P. *Lab Chip* **2009**, *9*, 2484-2494.

[9] Wilson, I. G. *Appl. Environ. Microbiol.* **1997**, *63*, 3741-3751.

[10] Abu Al-Soud, W.; Jonsson, L. J.; Radstrom, P. *J. Clin. Microbiol.* **2000**, *38*, 345-350.

[11] Abu Al-Soud, W.; Radstrom, P. *J. Clin. Microbiol.* **2001**, *39*, 485-493.

[12] Cabeen, M. T.; Jacobs-Wagner, C. *Nature reviews* **2005**, *3*, 601–610.

[13] http://www.qiagen.com, Qiagen QIAamp® DNA Mini and Blood Mini handbook.

[14] Hurley, S. S.; Splitter, G. A.; Welch, R. A. *J. Clin. Microbiol.* **1987**, *25*, 2227-2229.

[15] Shah, J. S.; Liu, J.; Buxton, D.; Stone, B.; Nietupski, R.; Olive, D. M.; King, W.; Klinger, J. D. *J. Clin. Microbiol.* **1995**, *33*, 322-328.

[16] Rantakokko-Jalava, K.; Jalava, J. *J. Clin. Microbiol.* **2002**, *40*, 4211–4217.

[17] Van Burik, J.; Schreckhise, R.; White, T.; Bowden, R.; Myerson, D. *Med. Mycol.* **1998**, *36*, 299–303.

[18] Sambrook, J.; Fritsch, E. F.; Maniatis, T. *Molecular cloning: a laboratory manual* Cold Spring Harbor Laboratory, Cold Spring Harbor, N.Y., 1989.

[19] Taylor, M. T.; Belgrader, P.; Furman, B. J.; Pourahmadi, F.; Kovacs, G. T. A.;

Northrup, M. A. *Anal. Chem.* **2001**, *73*, 492-496.

[20] http://www.cepheid.com, Xpert® MRSA 300-7258 Rev. B, June 2009.

[21] Mahalanabis, M.; Al-Muayad, H.; Kulinski, M. D.; Altman, D.; Klapperich, C. M. *Lab Chip* **2009**, *9*, 2811–2817.

[22] Yun, S. S.; Yoon, S. Y.; Song, M. K.; Im, S. H.; Kim, S; Lee, J. H.; Yang, S. *Lab Chip* **2010**, *10*, 1442-1446.

[23] Kim, J.; Jang, S. H.; Jia, G.; Zoval, J. V.; Da Silva, N. A.; Madou, M. J. *Lab Chip* **2004**, *4*, 516–522.

[24] Siegrist, J.; Gorkin, R.; Bastien, M.; Stewart, G.; Peytavi, R.; Kido, H.; Bergeron, M.; Madou, M *Lab Chip* **2010**, *10*, 363–371.

[25] Beckers, L. J. A.; Baragona, M.; Shulepov, S.; Vliegenthart, T.; van Doorn, A. R. *Proceedings of the 14th International Conference on Miniaturized Systems for Chemistry and Life Sciences, 2010, Groningen, The Netherland*, pp. 85-87.

[26] Grover, W. H.; Skelley, A. M.; Liu, C. N.; Lagally, E. T.; Mathies, R. A. *Sens. Actuators, B* **2003**, *89*, 315–323.

[27] Grover, W. H.; Ivester, R. H. C.; Jensen, E. C.; Mathies, R. A. *Lab Chip* **2006**, *6*, 623–631.

[28] The report on the full characterization of the isotropically-etched valve structure is in preparation.

[29] Schindler, C.; Schuhardt, V. *Proc. Natl. Acad. Sci. USA* **1964**, *51*, 414-421.

[30] Liu, R. H.; Yang, J.; Lenigk, R.; Bonanno, J.; Grodzinski, P. *Anal. Chem.* **2004**, *76*,

1824-1831.

[31] Beyor, N.; Yi, L.; Seo, T. S.; Mathies, R. A. *Anal. Chem.* **2009**, *81*, 3523-3528.

[32] Hwang, K. Y.; Lim, H. K.; Jung, S. Y.; Namkoong, K.; Kim, J. H.; Huh, N.; Ko, C.; Park, J. C. *Anal. Chem.* **2008**, *80*, 7786-7791.

[33] Hwang, K. Y.; Jeong, S. Y.; Kim, Y. R.; Namkoong, K.; Lim, H. K.; Chung, W. S.; Kim, J. H.; Huh, N. *Sens. Actuators, B* **2011**, *154*, 46-51.

[34] Hwang, K. Y.; Kim, J. H.; Suh, K. Y.; Ko, J. S.; Huh, N. *Sens. Actuators, B* **2011**, *155*, 422-429.

[35] Hou, K. US 6565749.

[36] Hou, K.; Gerba, C. P.; Goyal, S. M.; Zerda, K. S. *Appl. Environ. Microbiol.* **1980**, *40*, 892-896.

[37] Goyal, S. M.; Gerba, C. P. *Appl. Environ. Microbiol.* **1980**, *40*, 912-916.

[38] *ed.* Persing, D. H.; Tenover, F. C.; Versalovic, J.; Tang, Y.; Unger, E. R.; Relman, D. A.; White, T. J. *Molecular microbiology: diagnostic principles and practice*, ASM Press, Washington, D.C., 2004.

Chapter 5. Solid phase DNA extraction with flexible bead-packed microfluidic device to detect MRSA in nasal swab

5-1. Introduction

Since the concept of micro total analysis system (μTAS) proposed by Manz [1], microfluidics-based biomolecule analysis has been emerged as a promising approach to integrate both the complex analyte preparation and detection processes [2-5]. μTAS can provide numerous advantages over conventional laboratory methods such as ease-of-operation, increased detection sensitivity, low cost, and reduced time to result [1-8]. μTAS utilizes the interaction between a liquid solution containing target analyte and a solid surface because the analytical operations depend largely on the surface-based bioassays [9-16].

An approach to facilitate such interactions is to fabricate a solid support possessing a high surface-to-volume ratio (SVR) in microdevice [10]. In this way, the available surface area per unit volume for binding target analyte can be increased, thereby allowing for improved detection sensitivity and time-to-result *via* analyte enrichment and efficient mass transport. Various high SVR microstructures, such as beads, micropillars, porous polymer monolith, and membrane, have been installed into microfluidic devices [9-23]. Among them, beads have been widely employed in bioanalytical microdevices because

their surfaces can be easily modified with various materials with biological specificity such as silica, organosilane, protein (enzyme), and nucleic acid [9-18, 23-29]. To immobilize the beads inside a microchannel, an internal on-chip geometrical feature (frit or dam) [9-11, 18, 23, 32] or a magnetic field [9, 26-31] has been used. For the latter, it has been shown that the polymer magnetic beads with the size of submicrometers to several micrometers in a dilute suspension type could be easily manipulated for various purposes such as separation, mixing, and transport [9, 26-31]. For the non-magnetic type beads such as silica or glass, however, their application has been limited to a traditional stationary phase as can be seen in a chromatography column [9-16]. For this reason, the interaction between a liquid solution and a bead surface has been mostly utilized in a natural diffusion-based format. In this case, the mixing efficiency, which directly determines the performance of bioassays, would be less efficient than that of magnetic beads.

In addition to the aforementioned bead type, the close packing of beads into microchip is another issue to consider. Generally, the beads were transported to a localized region in microchip during an analytical testing after completing microchip fabrication [18, 25-28]. Notably, it becomes more challenging to prepare uniformly-packed beads with the increase of size and density of beads. For close-packing, it often necessitates the use of light polymer-based magnetic particles or a specialized microfluidic network so as to prevent the precipitation of beads from influencing both assay performance and solution transport. In this context, the direct introduction of beads

into a designated location during microchip fabrication can be an alternative to address such issues; it would simplify overall biological testing processes and facilitate uniform packing of large (> tens of micrometers) or heavy beads (*e.g.*, silica or glass beads). We have shown in our previous report [23] that dry surface-modified glass beads (*ca.* 40 μm) can be directly placed in a microchamber of a miniaturized bead-beating device that is equipped with weirs. The mechanical cell lysis was successfully demonstrated by utilizing the PDMS membrane valve as an actuator, which was pneumatically vibrated to cause bead collisions with shearing effect. In this study, we show that such a bead-beating platform can be significantly improved by adjusting the SVR for each solid phase extraction step. More importantly, the analytical validation on this platform is attempted by detecting MRSA strains in nasal swab samples. The present bead-packed chamber has a flexible PDMS wall to control its void volume. Such flexibility allows for reversible switching of the two packing states between random close packing (*i.e.*, high SVR) and loose packing (*i.e.*, low SVR) by deflecting the flexible wall upwards or downwards. Also, the cycling of these two states could induce vigorous mixing and disrupt the cell membrane even for gram-positive bacteria. Interestingly, the close packing of beads was highly reproducible and consistent (*i.e.*, invariant SVR) even with different bead amounts (10 ~ 16 mg). These additional dynamic characteristics to a typical stationary solid phase enabled the proposed microdevice to be more suitable for a series of solid phase extraction steps (binding-washing-eluting). By taking advantage of the above features, the analytical performance was evaluated by constructing the full detection schemes for

MRSA detection in nasal swab, such as nasal swab collection, pre-filtration for the removal of large impurities, on-chip DNA extraction, and real-time PCR. The current flexible microdevice yielded an excellent analytical PCR detection sensitivity of *ca.* 61 CFU/swab with 95% confidence interval, which was comparable to the commercial MRSA detection techniques.

5-2. Experimental

5-2-1. Cell strain and culture

MRSA strains used in this study were methicillin-resistant *staphylococcus aureus* ATCC BAA-1717 (MREJ type ii), NCTC 13395 (MREJ type v), and JCSC 3624 (MREJ type xii). They were grown in 50 mL trypticase soy broth (Becton, Dickinson and Company) at 37 ℃ overnight and suspended to appropriate concentrations after washing twice with 1X PBS solution (pH 7.4). The optical density of 0.2 OD was found to be *ca.* ~10^8 CFU (colony forming unit)/mL.

5-2-2. Device fabrication, testing instrumentation, and bead surface modification

The flexible bead-packed microdevice was fabricated by sandwiching a monolithic flexible PDMS membrane (thickness: ~250 μm) between two glass chips. Subsequently,

the surface-modified glass beads were directly introduced into a bead chamber of the top glass chip, and then the open bead chamber was covered with a rigid polycarbonate plate (*i.e.*, polycarbonate-glass-PDMS-glass) as shown in Figure 4-3. Microfluidic features such as valve seats and channels were fabricated on a glass wafer using conventional photolithography and wet etching techniques [23, 33-36]. The bead chamber was of an oval type and had the volume of *ca.* 15 μL and the size of *ca.* 6 mm × 4 mm × 0.75 mm (Longest × Shortest × Depth). The two pneumatic displacement chambers had the total volume of *ca.* 3 μL and the size of *ca.* 6 mm × 4 mm × 0.2 mm (Longest × Shortest × Depth). The PDMS membrane was operated by applying a positive or negative pressure in pneumatic displacement chambers through an array of solenoid valves (S070-5DC, SMC), which were interconnected with electro-pneumatic-regulator (ITV0030-3BL, SMC) and LabVIEW software (National Instruments). Glass beads (Polysciences) with diameters of 30 μm ~ 50 μm were coated with trimethoxysilylpropyl modified polyethyleneimine (Gelest) (see Supporting Information S1). Detailed descriptions of device fabrication, testing instrumentation, and bead surface modification were reported in our previous report [23].

5-2-3. Simulation of PDMS membrane deflection

To investigate the effect of PDMS membrane deflection on bead packing, a simple axisymmetric model for the microdevice was used as shown in Figure 5-1a. A uniform

pressure ($P_{pneumatic}$) load condition was set on the upper side boundary of PDMS membrane. Zero displacement condition in the y-direction was set on the left side boundary while zero displacement condition in both x- and y-directions was set on the lower side boundary. PDMS membrane thickness was fixed to be 250 μm while the chamber depth was varied from 10 to 100 μm.

The model was solved as a steady-state problem using Stress and Grid Deformation module in CFD-ACE+ (ver. 2009, ESI Group, France) with the pneumatic pressure being increased from 0 to 300 kPa at an increment of 10 kPa. The increment was reduced to 2 kPa in the initial state (0 ~ 10 kPa) and around the instant of contact between PDMS membrane and glass, as shown in Figure 5-1c. The increase of pneumatic pressure was terminated when any element with negative volume was generated. Standard first order element was used and the total number of nodes and elements were 3815 and 3649, respectively. The material properties [37] used for the simulation were as follows:

PDMS: density = 970 kg/m^3, Young's modulus of elasticity = 750 kPa, Poisson's ratio = 0.5.

Glass: density = 2520 kg/m^3, Young's modulus of elasticity = 80 GPa, Poisson's ratio = 0.3.

5-2-4. Cell releasing efficiency from swab

Two commercial swabs, flocked swab (Cat. No. 553C, Copan) and fiber swab (Cat.

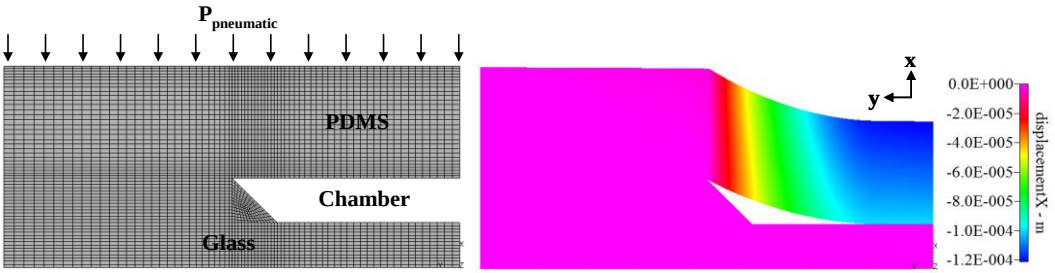

(a) (b)

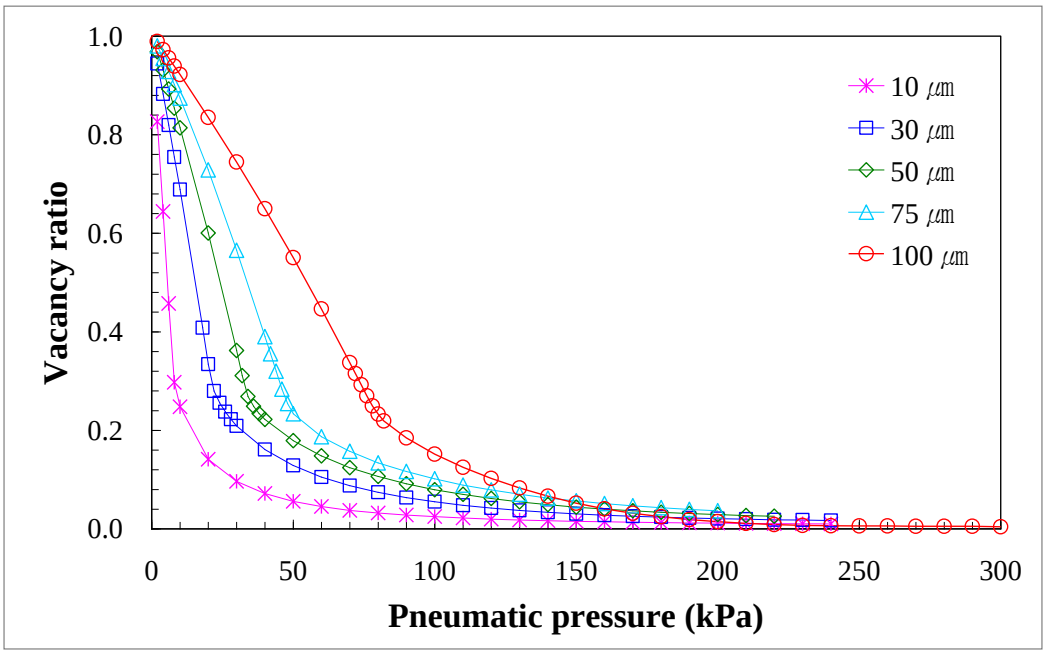

(c)

Figure 5-1. (a) Axisymmetric model for membrane deflection simulation (chamber depth = 100 μm). (b) Contour plot of displacement in the x-direction for $P_{pneumatic}$ = 100 kPa (chamber depth = 100 μm). (c) Vacancy ratio as a function of applied pneumatic pressure.

No. 220099, BBL™ CultureSwab™, BD), were tested to determine their cell releasing efficiency. The known concentration of MRSA suspension (1× PBS buffer, pH 7.4) was serially diluted to achieve concentration of ~ 10^3 CFU/mL. Its 100 μL aliquot was added to 900 μL of PBS buffer in 1.5 mL microcentrifuge tubes. It was spread on Petrifilm (3M, USA) as the initial MRSA cell number. A swab was soaked with 1 mL of MRSA suspension (~ 10^3 CFU/mL, the absorbed liquid volume was found to be *ca.* 100 μL) and then it was vortexed in 1 mL of fresh PBS buffer for 1 min. The solution with released MRSA was spread on Petrifilm as the recovered MRSA cell number. They were performed in triplicate with each swab and repeated for 3 different production lots. They were incubated at 37 ℃ for 24 h and colonies formed were counted. The cell releasing efficiency was calculated by dividing the number of recovered bacterial colonies by the number of initial bacterial colonies. The cell capture efficiency was similarly measured by counting colonies of solutions before and after passing through bead-packed device [19, 23].

5-2-5. DNA extraction from MRSA in nasal swab

Negative nasal swabs were pooled and spiked with MRSA for analytical testing as MRSA-positive sample. In details, dry flock swabs were used to collect specimen from the anterior nares of healthy volunteers. The collected swabs were pooled in sodium phosphate buffer (50 mM, pH 3, Sigma-Aldrich). Afterwards, they were vortexed for 1

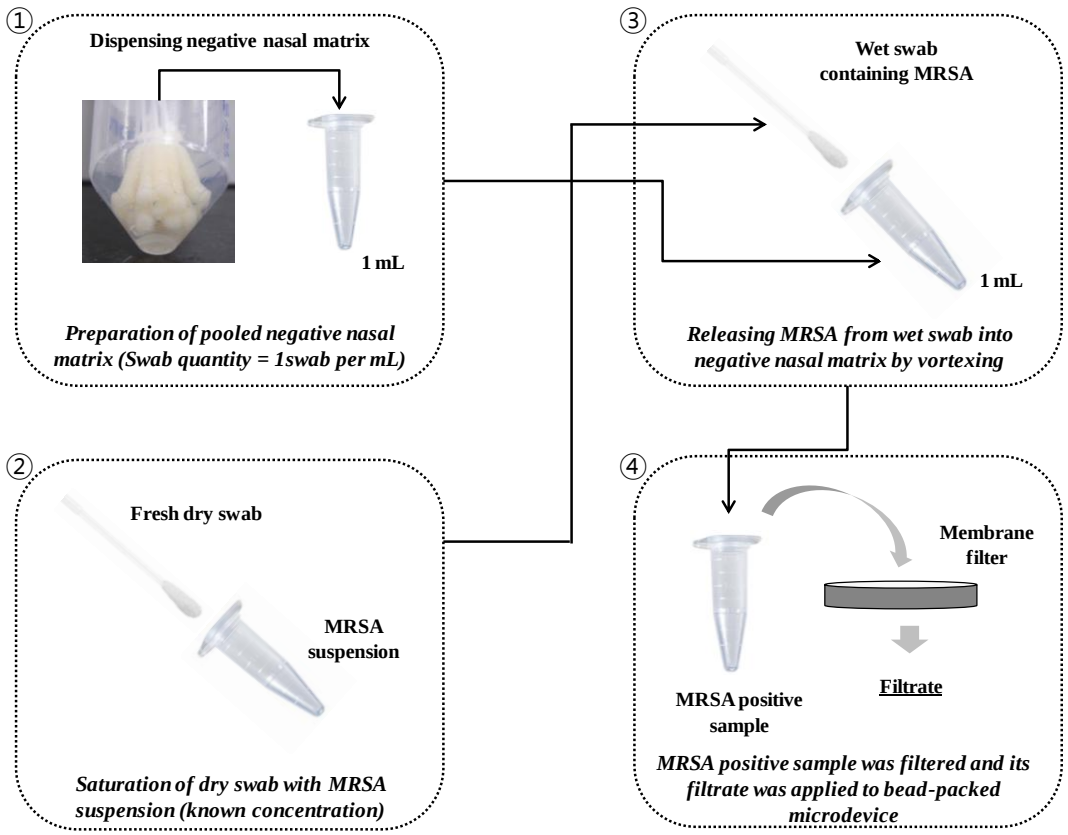

Figure 5-2. Nasal swab pretreatment steps for its application to flexible bead-packed microdevice.

min to simulate MRSA discharging (negative nasal matrix). The volume of negative nasal matrix was adjusted to be 1 swab per 1 mL. Another dry swab was soaked with known concentration of MRSA suspension as a simulated positive MRSA swab. The swab stem was broken and the absorbed MRSA was discharged in 1 mL of negative nasal matrix by vortexing. The resulting MRSA-positive nasal swab was passed through Isopore™ membrane filter with pore size of 3 μm (Millipore). The graphical description of nasal swab pretreatment steps was given in Figure 5-2. 1 mL of filtered MRSA-positive nasal swab, 0.5 mL of Tris-EDTA buffer (10 mM, pH 8, Ambion) for washing, and each 6 μL and 4 μL of NaOH solutions (0.02 N, Sigma-Aldrich) for lysis and DNA elution were previously dispensed into liquid reservoirs of testing module. The liquid solutions were transported in a pressure-driven manner and their operating fluid pressures were determined in preliminary experiments. The nasal swab solution passed through the bead-packed chamber with a flow rate of *ca.* 200 μL/min at *ca.* 50 kPa while pressurizing PDMS membrane of bead chamber upward at 150 kPa. After initial loading, the bead-packed chamber was washed at a flow rate of *ca.* 500 μL/min (80 kPa), and N_2-dried for 30 sec with 100 kPa while maintaining membrane upward. For lyzing the captured cells, 6 μL of NaOH was injected with the membrane downward, and valves at both sides of bead-packed chamber were closed. The pressures of two pneumatic displacement chambers alternate asynchronously with one chamber positive (80 kPa) and the other negative (-80 kPa) for the first half a cycle and they were reversed for the second half a cycle. The PDMS membrane vibrated at a frequency of 10 Hz for 5 min. The extracted

DNA was eluted by injecting another 4 μL of NaOH solution with a fluid pressure of 100 kPa with the membrane upward, and 10 μL of DNA solution was obtained as a result. The overall process took less than 20 min. No further DNA purification steps were performed. To measure the analytical sensitivity of the microdevice, at least 7 replicates were tested at each concentration (10, 20, 100, and 200 CFU/swab) for 3 types of MRSA strains. According to the number of positive calls made by PCR machine (*i.e.*, Ct cutoff value is 40), the analytical sensitivity with 95% confidence interval was predicted by statistical analysis using a probit regression model (MINITAB® Release 14.20).

The positive control samples (PTC) were prepared in order to compare their Ct value with those of the flexible microdevice. The MRSA suspension in PBS buffer was centrifuged at 13,200 rpm for 20 min and the supernatant was carefully discarded. The remained cell pellets were treated with table-top bead-beating instrument (GENIE 2, Fisher Scientific). After adding both 30 mg of bare glass bead and 10 μL of lysis solution (0.02N, NaOH) to the cell pellet, the vigorous vortexing was performed at the full speed for 5 min. The extracted DNA solution was recovered following brief centrifugation. For the accurate comparison, the injected cell number and the eluate volume were always controlled to be same with both methods.

5-2-6. Real-time PCR amplification

In order to evaluate the analytical performance, real-time PCR (polymerase chain

reaction) assays were performed on the LightCycler® 480 real-time PCR system (Roche). To identify MRSA, the sequence of junction regions of the staphylococcal chromosomal cassette (SCCmec) adjacent to the integration site, called SCC*mec* Right Extremity Junction (MREJ), and the *orfX* region was specifically amplified. Primer sets specific to MREJ type ii (forward: 5'- CGG GTT GTG TTA ATT GAA C - 3' and reverse: 5'- GAA GCG GCT GAA AAA ACC GCA - 3'), type v (forward: 5'- CGG GTT GTG TTA ATT GAA C - 3' and reverse: 5'- TAA AAT TAC GGC TGA AAT AAC CGC AT - 3'), and type xii (forward: 5'- CGG GTT GTG TTA ATT GAA C- 3' and reverse: 5'- ACA ATC CGT TTT TTA GTT TTA TTT ATG ATA CG - 3') were designed by Primer3 software (Whitehead Institute/MT Center for Genome Research), respectively. PCR reaction mixture (20 μL) was prepared to possess the following final concentrations: 0.4 μM TaqMan probe (FAM - 5' - aga Gca Ttt Aag Att Atg cg - 3' - BHQ1, LNA bases were indicated as capital characters, Sigma), 1 μM each primer (Sigma), 1x LightCycler® 480 Probes master mix (Roche), and 4 μL extracted DNA solution. After 10 min pre-denaturing step, the thermocycling was performed with a denaturation step at 95 ℃ for 20 sec and an extension step at 60 ℃ for 40 sec. The size of PCR amplicons were designed to be 91, 96, and 89 base pairs for MREJ type ii, v, xii, respectively. They were further confirmed by gel-electrophoresis (Agilent 2100 Bioanalyzer, Agilent Technologies).

5-3. Results and Discussion

5-3-1. Device operation

The bead-packed microdevice presented here is based on a monolithic flexible PDMS membrane valve between two glass layers [33-36]. The bead chamber (*ca.* 15 μL) with weirs was fabricated on the top glass wafer. After introducing dry surface-modified glass beads (30 μm ~ 50 μm) into the designated chamber, the top surface was covered with a rigid transparent PC plate for irreversible seal. Therefore, the device has a four-layer structure, PC-glass-PDMS-glass, as illustrated in Figure 4-3. The flexible wall was made of a PDMS membrane (250 μm thickness), which acted as a valving component as well as SVR regulating media for bead-packed chamber. Positive and negative pressures were applied to bend the flexible PDMS wall *via* pneumatic displacement of chambers in the bottom glass chip. The basic operation for solid phase DNA extraction is as follows (Figure 5-3): (1) cell capture on glass beads, (2) washing/drying, (3) lysis solution injection, (4) mixing along with bead-beating lysis, and (5) eluting the extracted DNA solution. When 16 mg of glass beads were used, for example, the SVR could be switched between 0.15 μm^{-1} (close packed) and 0.052 μm^{-1} (loose packed) to be well suited for each DNA extraction step. The PDMS membrane was deflected upwards when a high SVR is advantageous to increase interaction between liquid and solid surface such as binding (cell capture), washing, and eluting. Alternatively, it became downward to facilitate the injection of microscale liquid solution by increasing the void volume. The reversible switching and cycling between the two states was performed to induce

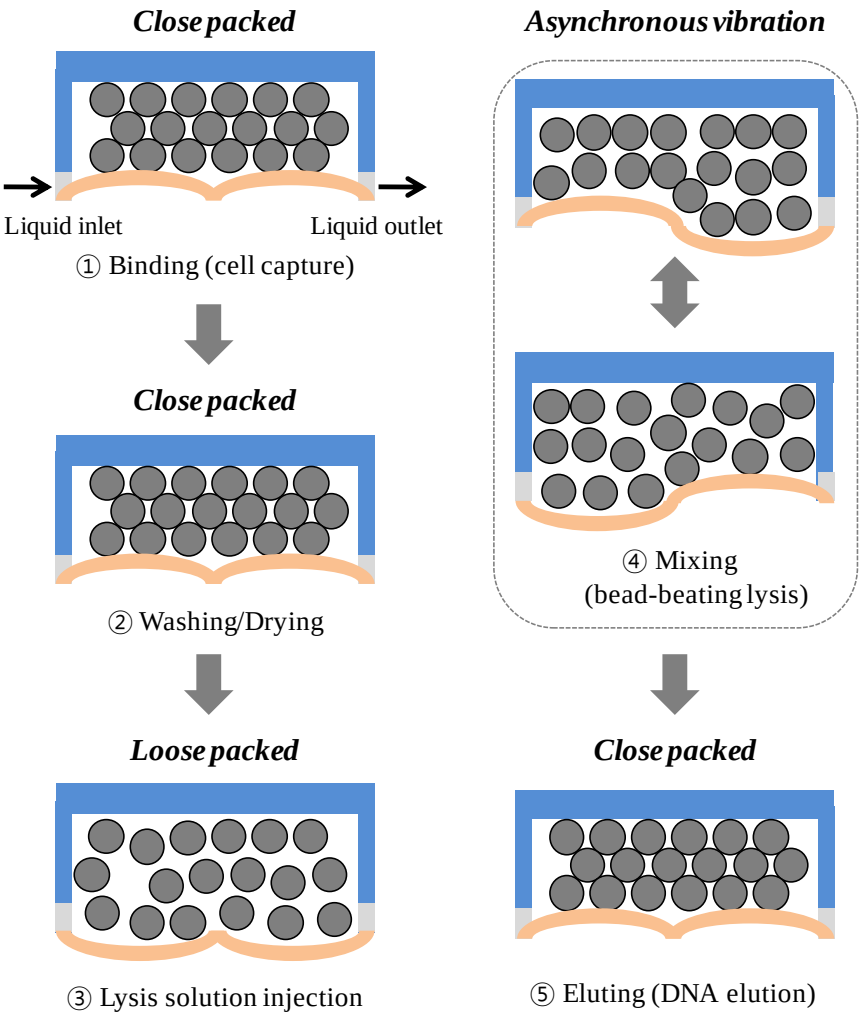

Figure 5-3. Membrane operation schematic for solid phase extraction processes such as binding, washing, and eluting step.

complete mixing of the beads with small liquid solution, thereby releasing the analyte (DNA) in a high concentration.

5-3-2. Pneumatically-actuated close packing of beads

We have investigated the deflection of PDMS membrane with commercial CFD-ACE+ simulation package to understand its effect on the close packing of beads. It was found that the deflection of PDMS membrane can displace the vacant chamber with a depth of 10 ~ 100 μm (Figure 5-1a). Here, the vacancy ratio was defined as the void volume that is not displaced by the PDMS membrane divided by the initial chamber volume. As shown in Figure 5-1c, the vacancy ratio was drastically decreased as the PDMS membrane was deflected without any contact with the chamber. Once the contact was made, the vacancy ratio was gradually decreased due to retarded deflection at the edge part of the PDMS membrane and generation of partial compression in the central part of the membrane. The vacancy ratio became less than 10% in most cases when the pressure was increased above 100 kPa (Figure 5-1c). These results indicated that the glass beads would be randomly close-packed by a pneumatic deflection of membrane.

Next, the cell capture efficiencies were measured for the two deflection states and three different bead amounts (Table 5-1). As the applied bead amount was decreased from 16 mg to 10 mg (*i.e.*, 38% reduction), the total bead surface area was proportionally decreased. Nonetheless, the SVR would be the same presumably even with 38 %

Table 5-1. Effect of the deflection of PDMS membrane on SVR (μm^{-1}) and cell capture efficiency (%) with different bead amounts (mg).

Bead amount (mg)	Upward		Rest	
	SVR (μm^{-1})	Capture efficiency (%)	SVR (μm^{-1})	Capture efficiency (%)
10	0.15	95.1 ± 1.2	0.05	37.2 ± 5.9
13	0.15	97.0 ± 1.3	0.08	60.8 ± 6.4
16	0.15	97.8 ± 0.6	0.11	87.2 ± 4.4

1 mL of MRSA (ATCC BAA-1717, 10^6 CFU/mL) in sodium phosphate (50 mM) was applied. Three repetitions were performed for each condition.

reduction of glass beads because the PDMS membrane could be more pressurized upwards with the reduced bead amount. Here, the SVR was calculated with two assumptions: uniform bead diameter (40 μm) and close packing ratio of 50%. When the PDMS membrane was deflected upwards, the cell capture efficiency and its standard deviation were found to be higher than those at rest. These results reveal that a higher SVR offers better assay performance by maximizing the interactions between liquid solution and bead surface. Owing to these characteristics, the operation of the flexible microdevice was highly consistent and reproducible even with different bead amounts as shown in Table 5-1.

5-3-3. Asynchronous membrane vibration for small volume elution

Until now, solid phase DNA extraction has been mostly performed on the stationary phase, so the target DNA was recovered by taking up time-dependent eluate fraction [11-12, 20]. Because the separation column is naturally stationary, the mass transport between liquid and solid support is only diffusion-based. Therefore, it has been difficult to release DNA from solid surface with a small elution volume (≤ 10 μL) efficiently for increased concentration, which is more compatible with downstream detection process such as PCR [11, 20, 30-31]. A dynamic solid phase DNA extraction based on rotating magnetic field was attempted to address this issue [30-31]. In our experiment, we performed vigorous mixing by vibrating the flexible PDMS membrane in an asynchronous manner (see

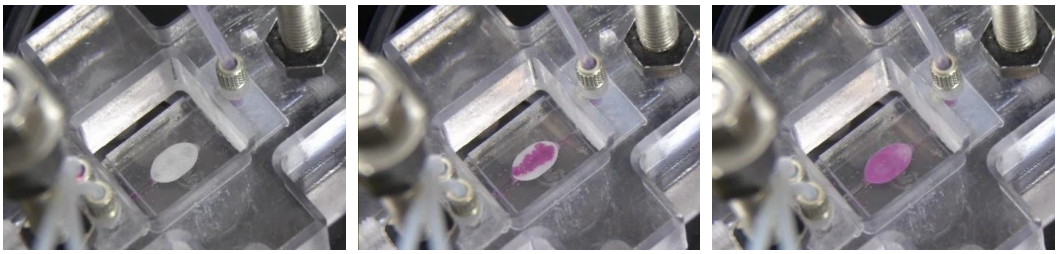

(a) (b) (c)

Figure 5-4. Mixing and bead-beating cell lysis through PDMS membrane vibration. (a) Before injecting liquid solution (close packed), (b) after injecting 6 µL of liquid solution (loose packed), (c) after cycling between two states (asynchronous vibration).

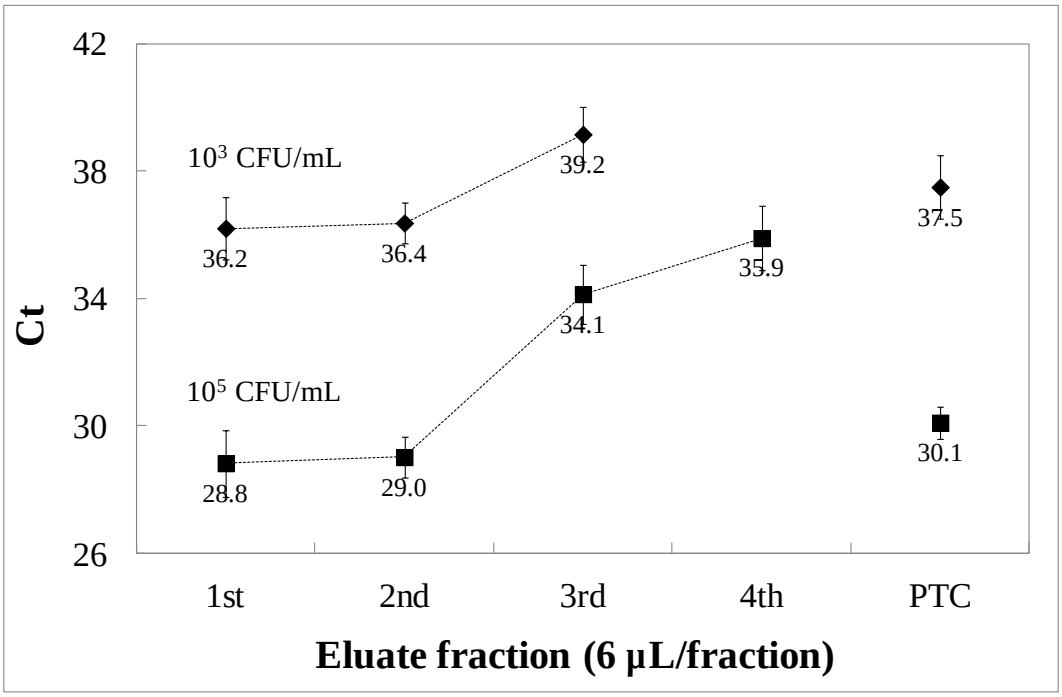

Figure 5-5. Ct values as a function of eluate fraction (0.02N NaOH). 1 mL of two different concentration of MRSA suspension (ATCC BAA-1717, 10^3 CFU/mL and 10^5 CFU/mL) was applied, respectively. 4^{th} fraction of 10^3 CFU/mL sample was not detected. PTC was obtained by centrifugation and subsequent table-top bead-beating lysis with 24 µL of NaOH solution. 1 µL of DNA solution was included in PCR as template. Three repetitions were performed for each condition.

experimental details and Figure 5-3④). In order to facilitate the injection of 6 μL NaOH solution for disrupting the adhered cells on the bead surfaces, the void volume of bead chamber was increased by *ca.* 3 μL with the membrane downward (Figure 5-3③). Then, the PDMS membrane was asynchronously vibrated to disrupt cell membrane as well as to release DNA (or cell) from the bead surface. For illustration purpose, such a dynamic mixing in a bead chamber was demonstrated with a colored ink as shown in Figure 5-4. To determine the DNA recovery rate from the captured cells, three additional liquid fractions (6 μL) were consecutively passed through after recovering the first 6 μL solution participating in membrane vibration. Each DNA amount was estimated by real-time PCR amplification. As shown in Figure 5-5, the Ct values of the first two fractions were lower than those of others by over 3 Ct difference. 10-fold difference in the initial DNA template copy numbers yields Ct change of *ca.* 3.3 when PCR efficiency is 100%. These results indicated that most of DNA (*ca.* 90%) could be eluted from the bead-packed chamber with initial 12 μL liquid solution. Therefore, a significant degree of 100-fold volume reduction (*i.e.*, from 1 mL of initial nasal swab sample to 10 μL of DNA eluate) would be translated into an increase in DNA concentration, which in turn results in an elevated detection sensitivity.

5-3-4. Detection of MRSA from nasal swab

MRSA is one of the most prevalent nosocomial or community-acquired infections all

over the world. It has been shown that early diagnosis and appropriate treatments could influence the patient stay length, morbidity, mortality rate, and preventative infection control in hospital [8]. Most of current diagnosis methods are culture-based, requiring 24-72 h to identify bacterial growth [38]. Thus, the molecular diagnostic method based on PCR has been employed to provide the improved detection sensitivity and fast time to result [8, 39]. The first step to detect MRSA is to collect the anterior nare specimen with swab and its discharging [40-42]. Two types of commercial swabs, regular fiber and flocked nylon, were evaluated for their cell releasing capability by measuring the colonies of released cells. Despite similar liquid absorption capacity (*ca.* 100 μL), they showed different cell releasing efficiency and lot-to-lot reproducibility as shown in Table 5-2. It was shown that the flocked swab yielded the consistent *ca.* 80% cell releasing efficiency with 3 production lots. In contrast, the fiber one exhibited lower efficiency with larger lot-to-lot variation. These results were in agreement with the report that the flocked swab has increased MRSA or SA detection rate in comparison with the fiber one when culturing nasal swab samples [43-44]. Based on these results, all subsequent experiments were performed with the flocked type swab.

Then, we established full DNA extraction processes for MRSA detection in nasal swab: swabbing, cell releasing from swab, pre-filtration and loading into flexible microdevice for DNA extraction. MRSA-spiked nasal swab was pre-filtered to prevent the device clogging caused by large impurities. The MRSA loss by pre-filtration was measured to be less than 10% as verified by colony count. The full processes from

Table 5-2. Cell releasing efficiency (%) and lot-to-lot variation according to swab type.

	Flocked type	Fiber type
Lot 1	81.7 ± 3.0	18.2 ± 4.9
Lot 2	77.7 ± 3.5	64.8 ± 1.4
Lot 3	88.5 ± 7.2	43.5 ± 8.2
Average	82.6 ± 5.4	42.2 ± 23.3

Three repetitions were performed for each condition.

swabbing to real-time PCR detection of MRSA were successfully performed with various MRSA concentrations as shown in Figure 5-6 (10^4, 10^3, and 10^2 CFU/swab). The extracted DNA was eluted with total 10 µL of NaOH solution and 4 µL out of it was included in PCR as with the positive control sample (PTC). The negative nasal matrix not spiked with MRSA was not amplified. PTC samples were prepared from MRSA suspension in PBS without MRSA releasing from swab and pre-filtration steps. When they were started from nasal swab as done with the microdevice, PCR amplification was significantly inhibited due to the concentrated impurities resulting from the centrifugation and subsequent lysis with small liquid volume (10 µL, data not shown). Such observation indicated that the flexible microdevice could remove the possible PCR inhibitors through flow-through cell capture and washing steps, and therefore detect MRSA in nasal swab successfully.

Finally, we attempted to estimate the analytical sensitivity, defined as the lowest number of CFU per swab that can be reproducibly distinguished from negative samples, by testing 3 types of MRSA strains (MREJ type ii, v and xii) at different cell concentrations (10, 20, 100, and 200 CFU/swab), respectively. As shown in Table 5-3, the analytical sensitivity was predicted to be *ca.* 47 ~ 61 CFU/swab with 95% confidence interval for the tested three strains. It was demonstrated that the flexible microdevice performed better than or similar to commercial MRSA detection methods. Such behavior was analyzed by investigating its analyte dilution ratio (ADR) in comparison with those of commercial methods. The ADR represented how much of analyte was included in final

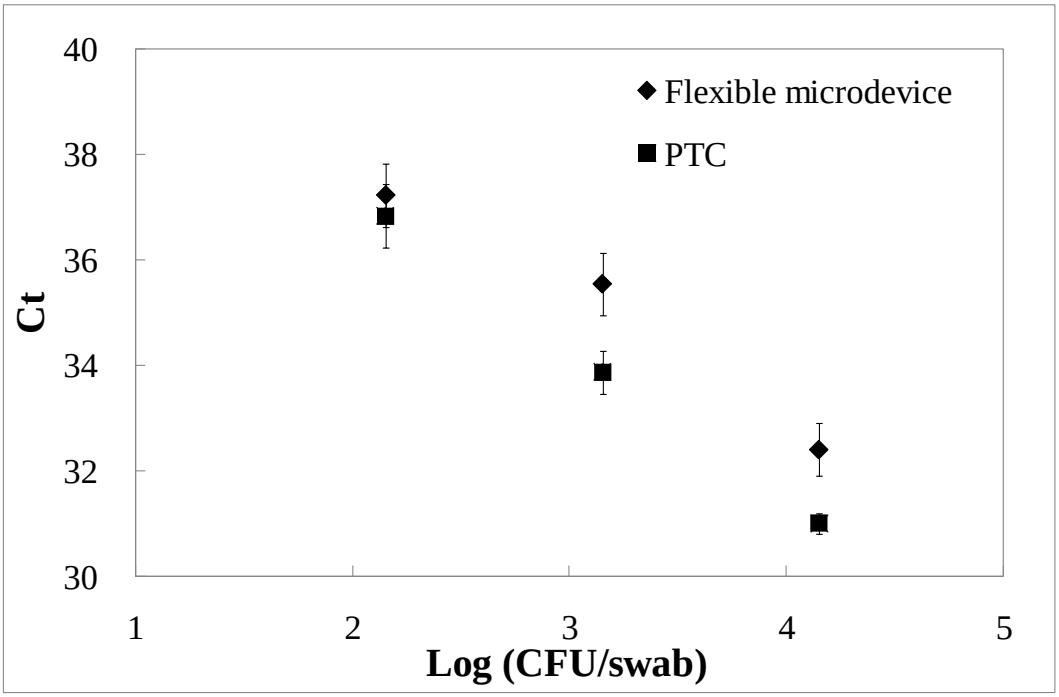

Figure 5-6. Detection of MRSA (NCTC 13395) from nasal swab as a function of initial cell number (CFU/swab). PTC was obtained by centrifugation and subsequent table-top bead-beating lysis with 10 µL of NaOH solution. 4 µL of DNA solution was included in PCR as template. Three repetitions were performed for each condition.

PCR (*i.e.*, the theoretical value of swab quantity per amplification reaction). Therefore, the ADR could be used as an index to describe theoretical analyte enrichment ratio of bioanalytical method. For example, the present microdevice processed 1 swab in 1 mL into 10 μL of eluate solution, and 4 μL out of it was included in PCR, yielding the ADR of 0.4 swab/PCR. This value appears higher than those of the existing methods by 1 ~ 2 orders-of-magnitude (see Table 5-3). This difference would result from the fact that other DNA preparation methods requiring multiple manual steps with traditional experimental tools (such as centrifuge, table-top bead-beating machine, pipet, heat block, and tube, *etc.*) [41-42] will dilute target analyte. Taking full advantage of the inherent microscale dimension of microdevice along with its dynamic properties of solid phase yielded such a high ADR value. The present SPE microdevice with flexible wall would facilitate microfluidic integration with a detection module because it was constructed based on a monolithic polymer membrane valve. Such characteristics would make this device a promising approach to DNA-based μTAS aimed for clinical diagnostics.

5-4. Summary

In this chapter, we have developed a flexible bead-packed microfluidic device to perform solid phase extraction of bacterial DNA from MRSA in nasal swab. The flexible PDMS membrane was pneumatically manipulated to control the SVR in the range of 0.05 to 0.15 (μm^{-1}), whose value was adjusted to be suitable for each DNA extraction step

Table 5-3. Estimated analytical sensitivity (CFU/swab, 95% confidence interval) for three MRSA strains and its comparison with other methods.

Methods	Analytical sensitivity (CFU/swab)			Analyte dilution ratio (Swab/PCR)
	MREJ type v[a]	MREJ type xii[b]	MREJ type ii[b]	
Flexible microdevice	54	47	61	0.4
Xpert® SA nasal complete [40]	97	127	256	-[c]
NucliSENS EasyQ® MRSA [41]	200	182	227	0.02
GeneOhm™ MRSA ACP Assay [42]	130	386	576	0.004

MRSA in swab (MRSA-positive swab) were released in buffer solution (Sodium phosphate, 50 mM)[a] or negative nasal matrix[b], respectively. [c]The details of biological testing protocols are not available. NucliSENS EasyQ® MRSA utilized a dry flocked swab and others did not specify the swab type.

such as cell capture, washing/drying, mixing (lysis), and eluting. It was shown that the fully deflected state of the membrane led to a constant SVR of 0.15 (μm^{-1}) even with the variation of bead amount (10 ~ 16 mg), allowing for consistent operation of the beat-beating device and highly improved capture efficiency (~97%). Moreover, the vigorous mixing by asynchronous membrane vibration yielded *ca.* 90% DNA recovery in *ca.* 10 μL of liquid solution. The full MRSA detection processes from nasal swab collection, DNA extraction on flexible microdevice, and real-time PCR amplification were established and validated by measuring the analytical sensitivity. This flexible microdevice provided an excellent analytical PCR detection sensitivity amounting to *ca.* 61 CFU/swab with 95% confidence interval, which turned out to be higher than or similar to those of the commercial DNA-based MRSA detection techniques. The proposed bead-packed microdevice with a flexible wall is potentially useful as a solid phase extraction method toward various sample-to-answer systems.

References

[1] Manz, A.; Graber, N.; Widmer, HM. *Sens. Actuators, B* **1990**, *1*, 244-248.

[2] Chen, L.; Manz, A.; Day, P. J. R. *Lab Chip* **2007**, *7*, 1413-1423.

[3] Ohno, K.; Tachikawa, K.; Manz, A. *Electrophoresis* **2008**, *29*, 4443-4453.

[4] West, J.; Becker, M.; Tombrink, S.; Manz, A. *Anal. Chem.* **2008**, *80*, 4403-4419.

[5] Kovarik, M. L.; Gach, P. C.; Ornoff, D. M.; Wang, Y.; Balowski, J.; Farrag, L.;

Allbritton, N. L.; *Anal. Chem.* **2012**, *84*, 516-540.

[6] Niemz, A.; Ferguson, T. M.; Boyle, D. S. *Trends in Biotechnology* **2011**, *29*, 240-250.

[7] Chin, C. D.; Linder, V.; Sia, S. K. *Lab Chip* **2007**, *7*, 41-57.

[8] Koydemir, H. C.; Kulah, H.; Ozgen, C.; Alp, A.; Hascelik, G. *Biosens. Bioelectron.* **2011**, *29*, 1-12.

[9] Verpoorte, E. *Lab Chip* **2003**, *3*, 60N-68N.

[10] Peterson, D. S. *Lab Chip* **2005**, *5*, 132-139.

[11] Wen, J.; Legendre, L. A.; Bienvenue, J. M.; Landers, J. P. *Anal. Chem.* **2008**, *80*, 6472-6479.

[12] Price, C. W.; Leslie, D. C.; Landers, J. P. *Lab Chip* **2009**, *9*, 2484-2494.

[13] Kim, J.; Jensen, E. C.; Megens, M.; Boser, B.; Mathies, R. A. *Lab Chip* **2011**, *11*, 3106-3112.

[14] Gervais, L.; de Rooij, N.; Delamarche, E. *Adv. Mater.* **2011**, *23*, H151–H176.

[15] Verch, T.; Bakhtiar, R. *Bioanalysis* **2012**, *4*, 177-188.

[16] Wu, D.; Qin, J.; Lin, B. *J. Chromatogr, A* **2008**, *1184*, 542–559.

[17] Cady, N. C.; Stelick, S.; Batt, C. A. *Biosens. Bioelectron.* **2003**, *19*, 59-66.

[18] Oleschuk, R. D.; Shultz-Lockyear, L. L.; Ning, Y.; Harrison, D. J. *Anal. Chem.* **2000**, *72*, 585-590.

[19] Hwang, K. Y.; Lim, H. K.; Jung, S. Y.; Namkoong, K.; Kim, J. H.; Huh, N.; Ko, C.; Park, J. C. *Anal. Chem.* **2008**, *80*, 7786-7791.

[20] Reedy, C. R.; Bienvenue, J. M.; Coletta, L.; Strachan, B. C.; Bhatri, N.; Greenspoon,

S.; Landers, J. P. *Forensic Sci. Int. Genetics* **2010**, *4*, 206-212.

[21] Hwang, K. Y.; Jeong, S. Y.; Kim, Y. R.; Namkoong, K.; Lim, H. K.; Chung, W. S.; Kim, J. H.; Huh, N. *Sens. Actuators, B* **2011**, *154*, 46-51.

[22] Hwang, K. Y.; Kim, J. H.; Suh, K. Y.; Ko, J. S.; Huh, N. *Sens. Actuators, B* **2011**, *155*, 422-429.

[23] Hwang, K. Y.; Kwon, S. H.; Jung, S. O.; Lim, H. K.; Jung, W. J.; Park, C. S.; Kim, J. H.; Suh, K. Y.; Huh, N. *Lab Chip* **2011**, *11*, 3649-3655.

[24] Melzak, K. A.; Sherwood, C. S.; Turner, R. F. B.; Haynes, C. A. *J. Colloid Interface Sci.* **1996**, *181*, 635-644.

[25] Verpoorte, E. *Electrophoresis* **2002**, *23*, 677–712.

[26] Gijs, M. A. M.; Lacharme, F.; Lehmann, U. *Chem. Rev.* **2010**, *110*, 1518–1563.

[27] Hayes, M. A.; Polson, N. A.; Phayre A. N.; Garcia, A. A. *Anal. Chem.* **2001**, *73*, 5896-5902.

[28] Beyor, N.; Yi, L.; Seo, T. S.; Mathies, R. A. *Anal. Chem.* **2009**, *81*, 3523-3528.

[29] Pan, X.; Zeng, S.; Zhang, Q.; Lin, B.; Qin, J. *Electrophoresis* **2011**, *32*, 3399–3405.

[30] Durate, G. R. M.; Price, C. W.; Littlewood, J. L.; Haverstick, D. M.; Ferrance, J. P.; Carrilho, E.; Landers, J. P. *Analyst* **2010**, *135*, 531-537

[31] Durate, G. R. M.; Price, C. W.; Augustine, B. H.; Carrilho, E.; Landers, J. P. *Anal. Chem.* **2011**, 8*3*, 5182-5189.

[32] Kim, S. M.; Lee, S. H.; Suh, K. Y. *Lab Chip* **2008**, *8*, 1015-1023.

[33] Grover, W. H.; Skelley, A. M.; Liu, C. N.; Lagally, E. T.; Mathies, R. A. *Sens.*

Actuators, B **2003**, *89*, 315–323.

[34] Grover, W. H.; Ivester, R. H. C.; Jensen, E. C.; Mathies, R. A. *Lab Chip* **2006**, *6*, 623–631.

[35] Jensen, E. C.; Bhat, B. P.; Mathies, R. A. *Lab Chip* **2010**, *10*, 685–691.

[36] Li, Y.; Jones, W.; Rasti, F.; Blaga, I.; Bogdan, G.; Eberhart, D.; Kobrin, B.; Lee, D.; Nielsen, B. ; van Gelder, E.; Jovanovich, S.; Stern, S. *Lab Chip* **2011**, *11*, 2541.

[37] Good, B. T.; Reddy, S.; Davis, R. H.; Bowman, C. N. *Sens. Actuators, B* **2007**, *120*, 473–480.

[38] Klonoski, J.; Mondesire, R.; Rea, L.; Ward, D. C.; Jenison, R. D. *Anal. Biochem.* **2010**, *396*, 284-289.

[39] Lindsey, W.C.; Woodruff, E. S.; Weed, D.; Ward, D. C.; Jenison, R. D. *Diagn. Microbiol. Infect Dis.* **2008**, *61*, 273-279.

[40] Cepheid, Xpert® SA nasal complete, package insert, 300-8799 Rev. C.

[41] bioMerieux, NucliSENS EasyQ® MRSA, FDA 510K (K102740).

[42] BD Diagnostics, GeneOhm™ MRSA ACP Assay, FDA 510K (K093346).

[43] Jones, G.; Matthews, R.; Cunningham, R.; Jenks, P. *J. Clin. Microbiol.* **2011**, *49*, 2717-2718.

[44] Verhoeven, P.; Grattard, F.; Carricajo, A.; Pozzetto, B.; Berthelot, P. *J. Clin. Microbiol.* **2010**, *48*, 4242-4244.

국문초록

분자진단을 위한 박테리아 핵산 추출 방법 및 미세유체 디바이스를 개발하였다. 전통적인 복잡한 핵산준비과정을 마이크로 디바이스상에 구현하기 위하여, 세포포획, 세척, 파쇄, 핵산용출의 단계로 구성되어 있는 고체상 핵산 추출 방법이 제시되었다. 상기 방법을 통하여 다양한 인간 검체로부터 감염성병원균의 포획에서부터 핵산 추출까지의 전과정이 하나의 마이크로 칩에서 구현 가능하다는 것을 입증하였다.

먼저, 고체상 유체통과형의 마이크로 디바이스의 표면에 박테리아의 포획을 유도하기 위하여, 열역학적으로 유리한 디바이스 표면의 표면장력 및 용액 pH 를 최적화하였다. 표면개질된 실리콘 필라어레이를 제작하였고, 박테리아 세포를 흘려서 세포포획 효율을 측정하였다. 고속의 유체 흐름 속에서도 (400 μL/min) 버퍼용액에 존재하는 다양한 박테리아 종류 (*E. coli*, *S. epidermis* 그리고 *S. mutans*) 에 대해 75% 이상의 포획효율을 보였다. 또한, 50% 전혈 속에서도 박테리아 세포포획이 가능함을 증명하였다. 디바이스 표면에 포획된 세포는 바로 파쇄 후 용출되었고, 용출된 핵산은 PCR 방법을 통하여 성공적으로 증폭되었다.

다음으로, 저가의 일회용 마이크로 디바이스를 제작하기 위하여, 높은 단위 부피당 면적비 (0.152 μm^{-1}) 를 갖는 마이크로 필라어레이를 전기도금된 니켈 몰드를 이용하여 PMMA 기판상에 엠보싱 방법으로 제작하였다. 필라어레이의 표면을 실리콘옥사이드와 유기실란 물질로 연속적으로 코팅을 하였다. 필라와

PDMS 상판과의 결합을 가능케 하기 위하여, 필라의 상부면만을 광촉매/자외선 처리를 통해 유기막을 실온에서 선택적으로 제거하였다. 결과적으로 세포의 포획에 사용되는 필라 측면의 유기실란막 손실없이, 필라상부 유기막 아래에 있는 실리콘산화물층을 선택적으로 노출시켰다. 플라즈마 처리된 PDMS 상판을 결합합으로써 디바이스를 완성하였다. 제조 대량화 및 집적화를 위해 폴리머 엠보싱, 유기실란 코팅, 그리고 결합의 전과정이 6인치 웨이퍼 레벨에서 수행되었다. 제조된 PDMS/PMMA 칩을 이용하여 박테리아 핵산 추출을 수행하였고, 기존의 Glass/Si 칩과 세포 포획 효율 및 PCR 과의 호완성 면에서 유사한 성능을 보였다.

그리고, 그람양성 박테리아로부터 핵산 추출이 가능한 소형화된 비드비팅 디바이스를 개발하였다. 이 미세유체 디바이스는 두개의 유리웨이퍼 사이에 하나의 유연한 PDMS 막을 샌드위치 형태로 결합하여 제작하였다. PDMS 막은 공압을 이용한 진동을 통하여 추가적인 파쇄기기 없이 비드의 충돌을 일으키는 액츄에이터로서의 역할을 수행하였다. 1 mL 의 초기샘플에 있는 그람 양성세균인 황색포도상구균 혹은 메티실린 내성 황색포도상구균은 표면 개질된 비드 표면에 포획되고, 비드 비팅방법으로 파쇄된 후, 10 μL 혹은 20 μL 의 핵산 용액형태로 용출되었다. 상기 핵산용액을 이용하여 실시간 PCR 을 성공적으로 수행하였다. 한정된 비드 챔버내에 존재하는 액체의 부피비가 PDMS 막의 휨과 비드의 움직임을 결정하여, 세포파쇄 효율에 중요한 역할을 한다는 것이 밝혀졌다. 본 소형화된 비드 비팅 방법은 대부분의 황색포도상구균을 3 분내에 파쇄하였으며, 이 효율은 전통적인 보텍싱 기계

혹은 효소를 이용한 세포파쇄 방법과 유사하였다. 유효한 세포 농도는 초기부피의 감소효과로 인해 50 혹은 100 배 증가하였다. 이러한 분석체의 농축 및 효과적인 비드 비팅 방법은 그람 양성 박테리아에 대해서도 46 CFU 에 이르는 우수한 PCR 검출 민감도를 이루게 하였다.

마지막으로, 상기의 내부에 유연한 PDMS 벽을 갖는 비드 충진 미세유체 디바이스를 비강스왑으로부터 메티실린 내성 황색포도상구균 핵산추출을 자동화하는데 적용하였다. 유연한 PDMS 막이 비드 충진 챔버의 벽으로 사용함에 따라, 단위 부피당 면적비를 0.05 에서 0.15 μm^{-1} 범위에서 조절이 가능하게 됨으로써, 결합/세척/용출로 이루어진 고체상 추출 프로토콜의 원활한 수행을 할 수 있었다. 특히, 공압의 도움으로 이루어진 비드의 밀집 패킹은 10 ~ 16 mg 의 비드량 변화에서 일정한 단위 부피당 면적비 (0.15 μm^{-1}) 를 가져왔고, 이것은 디바이스의 재현성있는 작동 및 향상된 세포포획 효율을 이루게 했다. 또한, PDMS 막의 비동기적 진동에 의한 활발한 믹싱 방법은 10 µL 액체 용액으로도 비드 표면에 포획된 세포에서 90% 이상의 핵산 회수가 가능함을 보였다. 비강 스왑으로부터 메티실린 내성 황색포도상구균을 검출하기 위한 전 과정, 즉, 비강 스왑 수집, 여과, 칩상 핵산 추출, 그리고 실시간 PCR 검출이 성공적으로 확립되었다. 개발된 유연한 마이크로 디바이스는 95% 신뢰수준에서 스왑당 61 CFU 의 PCR 검출 민감도를 보였고, 이 민감도는 시장에 판매되고 있는 핵산 기반의 검출기술보다 비슷하거나 우수하다. 이러한 우수한 성능은 1 mL 이라는 대용량의 초기 샘플에서 마이크로 스케일 부피 (10 µL) 로 농축할 수 있는 유연한 비드 충진

디바이스의 특징에 기인한다고 할 수 있다. 본 논문에서 제안된 마이크로 디바이스는 고체상 추출방법으로써 다양한 마이크로 타스 구현에 적용될 수 있을 것이다.

주요어: 고체상 추출, 세포 포획, 표면 개질, 용액 통과형, 비드 비팅 파쇄, 단위 부피당 면적 비, 비드 충진된 유연한 마이크로디바이스

학번: 2009-30955